

Fasting-sensitive SUMO-switch on Prox1 controls hepatic cholesterol metabolism

Ana Jimena Alfaro^{1,2,3} , Claudia Dittner⁴ , Janina Becker⁴, Anne Loft^{1,2,3,5}, Amit Mhamane^{1,2,3}, Adriano Maida^{1,2,3}, Anastasia Georgiadi^{1,2,3}, Foivos-Filippos Tsokanos^{1,2,3}, Katarina Klepac^{1,2,3}, Claudia-Eveline Molocea^{1,2,3}, Rabih El-Merahbi^{1,2,3}, Karsten Motzler^{1,2,3} , Julia Geppert^{1,2,3}, Rhoda Anane Karikari^{1,2,3}, Julia Szendrodi^{2,3}, Annette Feuchtinger⁶, Susanna Hofmann⁷, Samir Karaca⁸, Henning Urlaub^{8,9}, Mauricio Berriel Diaz^{1,2,3}, Frauke Melchior⁴  & Stephan Herzig^{1,2,3,10,*} 

Abstract

Accumulation of excess nutrients hampers proper liver function and is linked to nonalcoholic fatty liver disease (NAFLD) in obesity. However, the signals responsible for an impaired adaptation of hepatocytes to obesogenic dietary cues remain still largely unknown. Post-translational modification by the small ubiquitin-like modifier (SUMO) allows for a dynamic regulation of numerous processes including transcriptional reprogramming. We demonstrate that specific SUMOylation of transcription factor Prox1 represents a nutrient-sensitive determinant of hepatic fasting metabolism. Prox1 is highly SUMOylated on lysine 556 in the liver of ad libitum and refed mice, while this modification is abolished upon fasting. In the context of diet-induced obesity, Prox1 SUMOylation becomes less sensitive to fasting cues. The hepatocyte-selective knock-in of a SUMOylation-deficient Prox1 mutant into mice fed a high-fat/high-fructose diet leads to a reduction of systemic cholesterol levels, associated with the induction of liver bile acid detoxifying pathways during fasting. The generation of tools to maintain the nutrient-sensitive SUMO-switch on Prox1 may thus contribute to the development of “fasting-based” approaches for the preservation of metabolic health.

Keywords Bile acids; Cholesterol; Liver; Prox1; SUMOylation

Subject Categories Metabolism; Post-translational Modifications & Proteolysis

DOI 10.1525/embr.202255981 | Received 17 August 2022 | Revised 12 July

2023 | Accepted 27 July 2023 | Published online 10 August 2023

EMBO Reports (2023) 24: e55981

Introduction

Hepatic metabolism critically regulates systemic energy homeostasis, in part by controlling the adaptation response during variations in nutrient availability and detoxification processes. Hepatocytes have evolved to sense and react to dietary signals through a network of nutrient sensing and signal transduction pathways in order to cope with the fluctuating energy demands (Panda *et al.*, 2002; Si-Tayeb *et al.*, 2010; Bechmann *et al.*, 2012; Juza & Pauli, 2014).

Physiological cues such as fasting and feeding signals are translated into specific transcriptional metabolic programs, which enable long-term regulation and adaptation of cellular metabolism. The activity of key regulatory factors, including transcription factors, is modulated by reversible post-translational protein modifications, which allows for fast adaptive responses to changes in the cellular environment. The regulatory network driven by post-translational modifications in response to metabolic cues has mainly been studied in the context of phosphorylation. However, one of the post-translational modifications that is gaining attention as a key regulator of transcription is SUMOylation.

SUMOylation refers to the enzymatic formation of an isopeptide bond between the 11 kDa small ubiquitin-like modifier (SUMO) and lysine residues of its target proteins with the help of E1, E2, E3 enzymes and ATP. Like phosphorylation, SUMOylation is reversible and highly dynamic. Deconjugation is catalyzed by several highly active SUMO-specific isopeptidases (Matunis *et al.*, 1996; Mahajan *et al.*, 1997; Geiss-Friedlander & Melchior, 2007; Vertegaal, 2022). The conjugation of SUMO occurs at lysine residues frequently within a SUMO-consensus motif (YKxE), a recognition site for the

1 Institute for Diabetes and Cancer, Helmholtz Munich, Neuherberg, Germany

2 Joint Heidelberg-IDC Translational Diabetes Program, Inner Medicine 1, Heidelberg University Hospital, Heidelberg, Germany

3 German Center for Diabetes Research (DZD), and German Center for Cardiovascular Disease (DZHK), Neuherberg, Germany

4 Zentrum für Molekulare Biologie der Universität Heidelberg (ZMBH), Heidelberg University, DKFZ-ZMBH Alliance, Heidelberg, Germany

5 Center for Functional Genomics and Tissue Plasticity (ATLAS), SDU, Odense, Denmark

6 Research Unit Analytical Pathology, Helmholtz Munich, Neuherberg, Germany

7 Institute of Diabetes and Regeneration Research, Helmholtz Munich, Neuherberg, Germany

8 Bioanalytical Mass Spectrometry Group, Max Planck Institute for Multidisciplinary Sciences, Göttingen, Germany

9 Bioanalytics, Institute of Clinical Chemistry, University Medical Center Göttingen, Göttingen, Germany

10 Chair Molecular Metabolic Control, Technical University Munich, Munich, Germany

*Corresponding author. Tel: +49 89 3187 1045; E-mail: stephan.herzig@helmholtz-munich.de

E2 conjugating enzyme (Gareau & Lima, 2010; Vertegaal, 2022). Mammals express two SUMO families, SUMO1 and SUMO2/3. Although conjugated via the same enzymatic pathway, the SUMO1 and SUMO2/3 isoforms share only around 50% of their amino acid sequence. Consistent with the differences observed between the amino acid sequences, SUMO1 and SUMO2/3 have overlapping and distinct mechanistic functions and may exert different consequences on the target protein (Tatham *et al.*, 2001; Di Bacco *et al.*, 2006; Zhu *et al.*, 2009; Alegre & Reverter, 2011; Chang *et al.*, 2011). Similar to phosphorylation, SUMOylation serves as a molecular switch controlling an array of cellular processes. The attachment of SUMO can generate new binding interfaces or block a binding site, thereby modulating the function of the target protein (Geiss-Friedlander & Melchior, 2007; Flotho & Melchior, 2013; Vertegaal, 2022). By promoting alterations in nuclear localization, preventing protein degradation, changing DNA binding affinity and regulating the interaction with chromatin modifying complexes, SUMOylation controls the activity of transcription factors and co-regulators, thus playing a crucial role in the dynamic regulation of transcription (Treuter & Venetclef, 2011; Rosonina *et al.*, 2017; Boulanger *et al.*, 2021).

Recent developments in SUMO-proteome analysis led to the identification of several thousand proteins that are under control of SUMOylation, including a vast number of transcription factors and transcriptional regulators (Hendriks & Vertegaal, 2016; Boulanger *et al.*, 2021). Previous studies have demonstrated that SUMOylation participates in the regulation of liver metabolism by controlling the activity of key hepatic transcription factors (Balasubramaniyan *et al.*, 2013; Lee *et al.*, 2014; Stein *et al.*, 2014; Kim *et al.*, 2015).

Here, we aimed to identify the dynamic role of SUMOylation in the transcriptional control of liver metabolism in response to changes in nutrient availability. To this end, we performed an endogenous SUMO1 and SUMO2/3 -proteome analysis of the mouse liver in the fasted and refeeding cycle. We identified the fasting-sensitive SUMOylation of the transcription factor Prox1 as a major SUMOylation event in the liver and as a key determinant of systemic cholesterol metabolism. The SUMO-switch on Prox1 allows the regulation of a distinct subset of genes involved in the hepatic cholesterol detoxification system in response to fasting. Our study provides the first example of a fasting-feeding sensitive post-translational modification with immediate functional impact on physiological responses to changes in environmental conditions.

Results

Prox1 is modified by SUMO at lysine 556 in response to nutrient availability

In order to define the hepatic SUMO-proteome in response to changes in nutrient availability, we extracted endogenous SUMO targets from liver tissue of fasted (16 h) and refed (fasted 16 h and refed 2 h) wild-type mice using monoclonal anti-SUMO1 and anti-SUMO2/3 antibodies and subsequent peptide elution as described previously (Becker *et al.*, 2013; Barysch *et al.*, 2014). The isolated proteins were analyzed by mass spectrometry and over 200 SUMO candidates were identified (Dataset EV1). Several candidates were differentially modified between the fasted and refed states (Table 1); a schematic representation of the experimental setup is shown in Fig 1A.

The target showing the most notable difference was Prospero homeobox protein 1 (Prox1). Prox1 is a key transcription factor controlling liver development and metabolism. Prox1 expression is essential for hepatoblast migration and hepatocyte cell commitment (Sosa-Pineda *et al.*, 2000; Burke & Oliver, 2002; Dudas *et al.*, 2004; Lu *et al.*, 2021; Velazquez *et al.*, 2021). In the adult liver, Prox1 controls key aspects of lipid metabolism. Adult mice lacking Prox1 in hepatocytes show a strong degree of liver steatosis and hepatic injury (Armour *et al.*, 2017; Goto *et al.*, 2017). Several studies have reported Prox1 to be a corepressor of key hepatic nuclear receptors and transcription factors such as the pregnane X receptor (PXR; Nr1i2, also known as SXR for steroid and xenobiotic receptor), liver receptor homolog-1 (LRH-1; Nr5a2), hepatocyte nuclear factor 4 α (HNF4 α), and estrogen-related receptor α (ERR α) (Qin *et al.*, 2004; Charest-Marcotte *et al.*, 2010; Azuma *et al.*, 2011; Dufour *et al.*, 2011; Stein *et al.*, 2014; Armour *et al.*, 2017). In addition, the transcriptional activity of Prox1 has been shown to be modulated by the attachment of SUMO1 in endothelial cells (Shan *et al.*, 2008; Pan *et al.*, 2009; Banerjee *et al.*, 2023).

Our mass spectrometry data indicated that Prox1 was substantially SUMOylated in the refed state with a paralog preference for SUMO2/3 over SUMO1, while Prox1 SUMOylation was weak during fasting (Fig 1A). To confirm these results, we performed a SUMO2 immunoprecipitation using liver tissue from fasted and refed wild-type mice. Indeed, the conjugation of Prox1 to SUMO2 was higher in the refed state (Fig 1B). The SUMOylated species of Prox1 (approx. 120kDa) was easily detected by immunoblotting in liver lysates without prior enrichment (Fig EV1A). To further understand how Prox1 was modified in response to nutrient availability, we analyzed liver samples collected after various fasting or refeeding time points. The liver samples were collected using prefrozen forceps to avoid delayed tissue freezing and throughout the dark phase to avoid circadian off-target effects. At the beginning of the dark phase (time point = 0), 15% of the total Prox1 pool was modified by SUMOylation in ad libitum fed mice (Fig 1C). The conjugation of Prox1 with SUMO was lost after 3 h of fasting and Prox1 remained unmodified for the rest of the dark phase in fasted mice (Fig 1C). Upon refeeding, the levels of Prox1 SUMOylation were maintained with a tendency to increase over time, around 25% of the total Prox1 pool was modified by SUMOylation in refed mice (Fig 1C). The levels of Prox1 protein and mRNA levels were constant between the fasted and refed conditions and through the dark phase (Fig 1C). Changes in blood glucose and insulin levels as well as the expression of metabolic and circadian genes were measured to corroborate the nutritional state of the mice upon fasting and refeeding (Fig EV1B). These findings identified a SUMO-switch on Prox1 with a clear response to nutrient availability.

To gain more insight into the molecular regulation of Prox1 SUMOylation, we aimed to identify the SUMO target site of hepatic Prox1. There are two potential SUMOylation sites on Prox1, defined by two highly conserved SUMO-consensus motifs around lysine residues 353 and 556 (Shan *et al.*, 2008; Pan *et al.*, 2009); a schematic representation of Prox1 is shown in Fig 2A. SUMO-consensus motifs within disordered regions are preferentially targeted for SUMOylation (Pichler *et al.*, 2005; Hendriks *et al.*, 2018). Alphafold-based protein structure prediction (Jumper *et al.*, 2021; Varadi *et al.*, 2022) of mouse Prox1 suggested that lysine 353 is part of an α -helix, while lysine 556 resides within an unstructured region making it a better

Table 1. SUMOylated proteins in the mouse liver during fasting or refed states.

Protein/Experimental condition	SUMO1 fasted	SUMO1 refed	SUMO2 fasted	SUMO2 refed	Control fasted	Control refed	
RanGAP1	227	227	79	94	0	0	
PML	19	25	83	89	0	0	
Trim28	2	4	7	10	0	0	
Prox1	0	2	5	43	0	0	
Zinc finger and BTB domain-containing protein 20	6	14	16	20	0	0	
Insulin-like growth factor 2 receptor	45	27	37	8	0	0	
TCP-1-delta	8	1	0	0	0	0	
Glucose-6-phosphate translocase	4	0	0	0	0	0	
Basic helix-loop-helix protein 40	0	0	0	9	0	0	
N-CoR	0	0	0	2	0	0	
Rip140	0	0	0	5	0	0	

An immunoprecipitation using SUMO1 and SUMO2/3 antibodies was performed using liver tissue of fasted or refed mice according to (Becker *et al*, 2013; Barysch *et al*, 2014). The immunoprecipitated proteins were analyzed by LC–MS. The table shows the total spectrum count for selected proteins differentially modified between the fasted and refed states. For the complete table of all identified proteins, see Dataset EV1.

candidate for SUMO conjugation (Pichler *et al*, 2005; Hendriks *et al*, 2018). In line with this, lysine 556 has been identified as the main SUMOylation site of Prox1 using an E.Coli expression-modification system and in endothelial cells (Pan *et al*, 2009). Therefore, we investigated whether lysine 556 is also the main SUMOylation site of Prox1 in a hepatocyte cell model. To this end, we generated expression constructs coding for mouse wild-type Prox1 (wt), a lysine (K) 556 to arginine (R) mutant (K556R) as well as a glutamic acid (E) 558 to alanine (A) mutant (E558A). The K556R mutant lacks the target lysine while the E558A retains the target lysine but has a mutated SUMO-consensus motif and should lose the ability to interact with the SUMO E2 conjugating enzyme (Gareau & Lima, 2010; Vertegaal, 2022). The status of Prox1 SUMOylation was analyzed in HepG2 cells overexpressing the Prox1 constructs. Both the unmodified and the SUMOylated species of Prox1 were detected in cells expressing the wt Prox1 (Fig 2B). However, the conjugation of Prox1 with SUMO was abolished when the target lysine 556 was mutated or the surrounding SUMO-consensus motif was disrupted (Fig 2B), establishing lysine 556 as the main SUMOylation site on Prox1 in a hepatocyte cell model.

Furthermore, we considered the potential paralog preference for SUMO2 over SUMO1. For this, untagged mouse Prox1 (mProx1) was purified from HEK293T cells and used for *in vitro* SUMOylation assays. The purified mProx1 was incubated with purified SUMO loading enzymes together with either SUMO1 or SUMO2. The *in vitro* SUMOylation of Prox1 was more efficient with SUMO2 than with SUMO1 suggesting that the paralog preference for SUMO2 was an intrinsic property of Prox1, similar to other known SUMO2 targets such as USP25 or BLM (Meulmeester *et al*, 2008; Zhu *et al*, 2008; Fig 2C).

Given that Prox1 plays a key role in the regulation of liver lipid metabolism (Armour *et al*, 2017), we decided to investigate the behavior of the Prox1 SUMO-switch in the liver of mice coping with a lipid overload. For this, we analyzed the modified status of Prox1 in mice challenged with a high-cholesterol diet and in two models of diet-induced obesity.

To this end, adult wild-type male mice were fed with a 2% high-cholesterol diet for 6 weeks; a control diet with 0% cholesterol was used as control. Liver samples were collected 3 h into the dark phase in the fasted and refed states. The conjugation of Prox1 with SUMO was drastically impaired during fasting in the liver of mice fed the control (ctrl) or the high-cholesterol diet (chol 2%) to a comparable degree (Fig 3A). The levels of SUMOylated Prox1 were promoted by refeeding in both groups but were significantly higher in mice fed the control diet as compared to mice fed the high-cholesterol diet (Fig 3A). The expression of Prox1 was constant between both groups (Fig 3A). The body weight records, serum parameters, and the content of liver cholesterol are shown in Fig EV2A.

Next, to establish a first model of diet-induced obesity, we fed adult wild-type male mice with a 60% high-fat diet (HFD) for 8 weeks; a standard chow diet was used as a control. Liver samples were collected 3 h into the dark phase in the fasted and refed states. As observed previously, the conjugation of Prox1 with SUMO was drastically impaired during fasting and promoted during refeeding in the liver of lean mice (Fig 3B). In the liver of HFD-fed obese mice, the conjugation of Prox1 with SUMO was only mildly affected during fasting while it was still promoted during refeeding (Fig 3B). The levels of SUMOylated Prox1 during fasting were significantly higher in the liver of HFD-fed obese mice as compared to the lean controls, while no differences were observed during refeeding (Fig 3B). The expression of Prox1 was constant between both groups during fasting and refeeding (Fig 3B). The body weight records and serum parameters are shown in Fig EV2B.

In the second model, we fed adult wild-type male mice with a 45% high-fat +20% w/v fructose diet (HF/hfD) for 12 weeks; we selected this diet to induce a metabolic burden at the level of both lipid intake and *de novo* synthesis, a standard chow diet was used as a control. Liver samples were collected 3 h into the dark phase in the fasted and refed states. The conjugation of Prox1 with SUMO was significantly reduced upon fasting in the liver of lean mice, while it was not affected in the liver of HF/hfD-fed obese mice

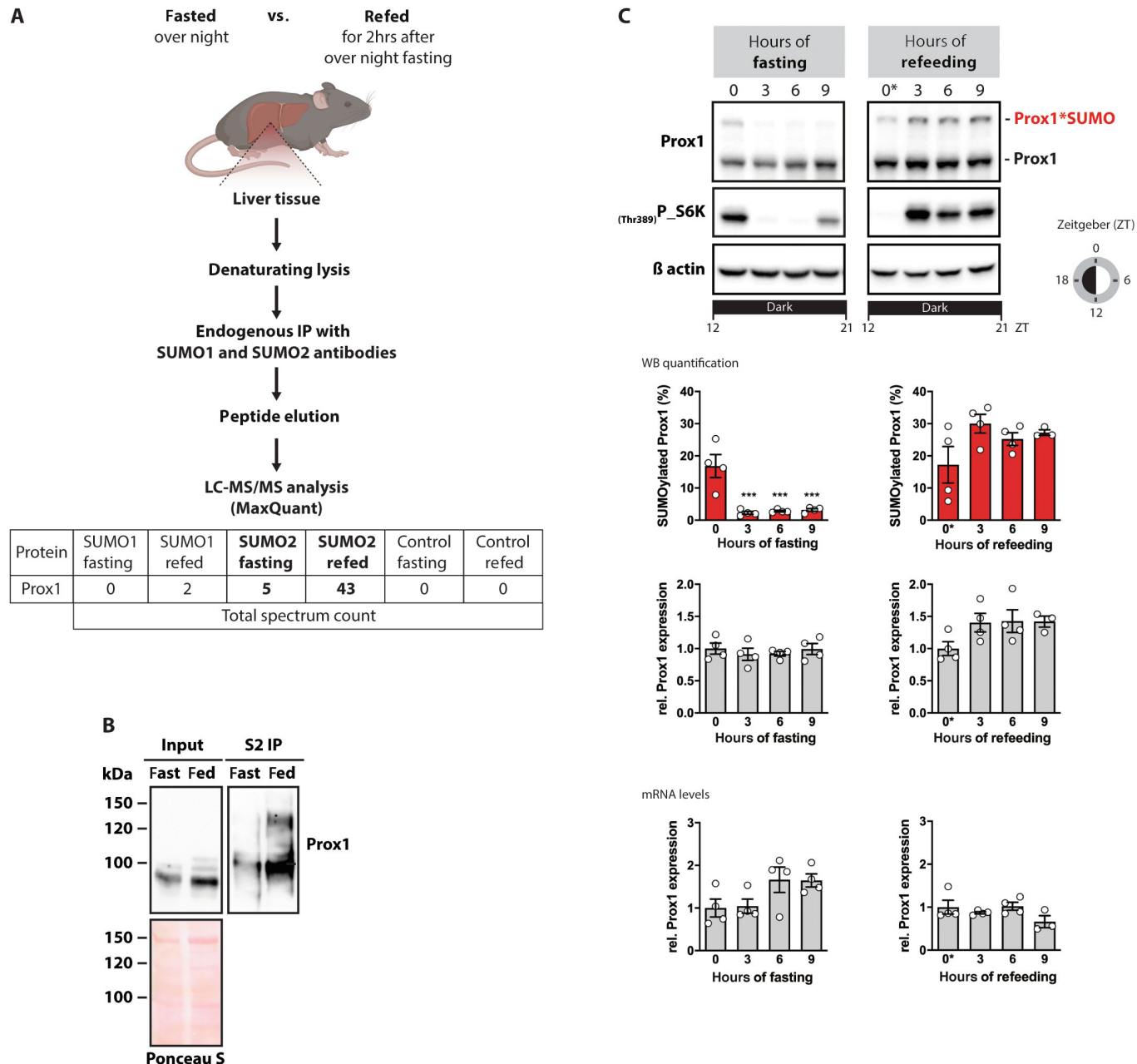


Figure 1. Hepatic Prox1 is modified by SUMOylation in response to nutrient availability.

- A Schematic representation of the protocol used to enrich and detect endogenous SUMO targets in the mouse liver in the fasted and refed states (Becker et al, 2013).
B SUMO2 immunoprecipitation using crosslinked SUMO2 antibody beads and liver samples of wild-type C57BL/6J mice in the fasted (16 h) or re-fed (16-h fasted and re-fed 2 h) states. Eluates analyzed by immunoblotting using anti-Prox1 antibodies and ponceau staining was used as loading control.
C 8 weeks old C57BL/6N male mice were fasted (food removed at ZT 12) or re-fed (fasted from ZT4 to ZT12 for synchronization; food re-introduced at ZT 12). Tissue samples were collected at ZT 12, 15, 18 and 21 ($n = 4$). Liver lysates analyzed by immunoblotting using anti-Prox1 and anti-P_S6K(Thr389) antibodies; β actin was detected as an input control.

The quantification of SUMOylated Prox1 (%) and total Prox1 protein expression as well as Prox1 mRNA levels analyzed by qPCR are shown. qPCR data are presented as relative fold change normalized to the housekeeping gene TBP.

Data information: Every dot represents one individual mouse. Data: mean \pm SEM. Significance was determined by one-way ANOVA with Dunnett's multiple comparison test relative to samples collected at ZT 12. ***P \leq 0.001.

Source data are available online for this figure.

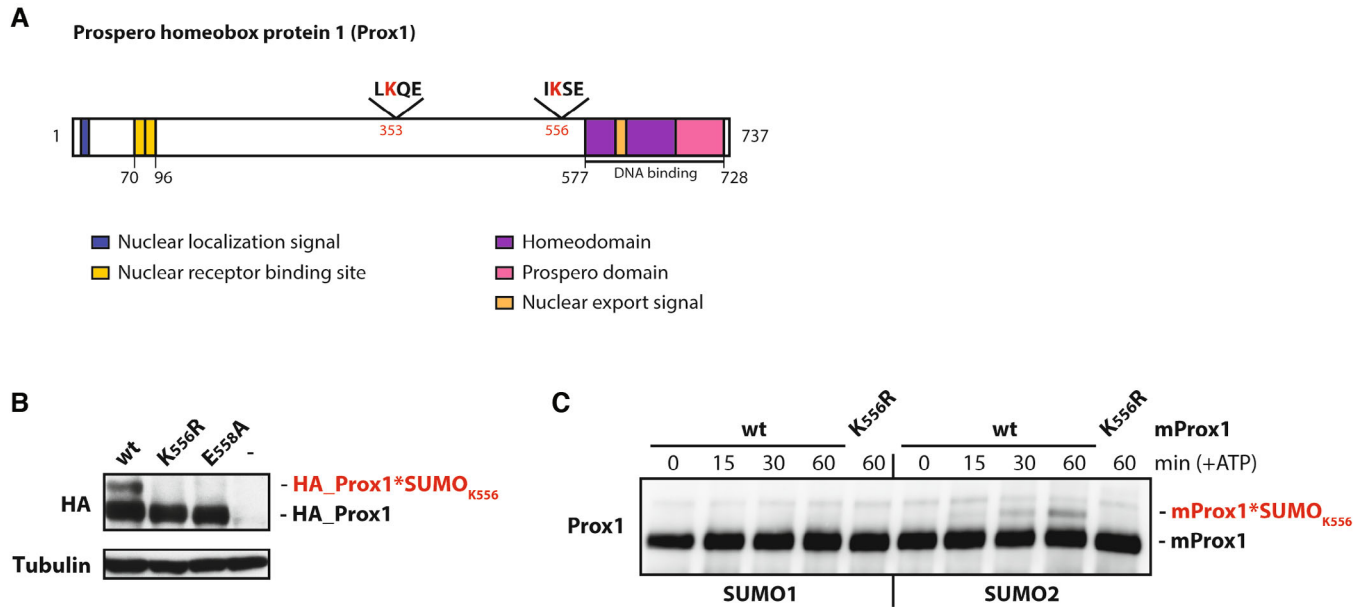


Figure 2. Prox1 is modified by SUMO2 on lysine residue 556.

- A Schematic representation of Prox1. Functional domains are highlighted. The two putative SUMO-consensus motifs ($\Psi K X E$) with SUMOylation sites at lysine (K) residues 353 and 556 are marked. Figure adapted from (Elsir et al., 2012).
- B HepG2 cells overexpressing HA-tagged mouse wild-type Prox1 (wt), Prox1 K556R mutant or Prox1 E558A mutant. Cell lysates analyzed by immunoblotting using anti-HA antibodies; tubulin was detected as an input control.
- C Mouse un-tagged Prox1 (mProx1) was purified from HEK293T cells. Purified mProx1 was incubated with recombinant E1 and E2 enzyme together with either SUMO1 or SUMO2. The enzymatic reactions were started with ATP and incubated for 15, 30 and 60 min. A reaction with the Prox1 K556R mutant (KR) was used as a control. The 0 min sample was incubated without ATP. Samples were analyzed by immunoblotting using anti-Prox1 antibodies.

Source data are available online for this figure.

(Fig 3C). The levels of Prox1 SUMOylation during fasting were significantly higher in the liver of obese mice as compared to the lean controls, while no differences were observed during refeeding (Fig 3C). The expression of Prox1 was constant between both groups (Fig 3C). The body weight records and serum parameters are shown in Fig EV2C.

These results demonstrated that the response of the Prox1 SUMO-switch to nutrient deprivation was altered under high-fat dietary stress conditions while isolated high-cholesterol exposure did not impair the physiological fasting-feeding response of Prox1 SUMOylation.

Liver-specific loss of lysine 556 SUMOylation on Prox1 decreases systemic cholesterol levels

The findings described above raised the question whether the SUMO-switch on Prox1 was functionally required for hepatic metabolism, particularly during high-fat dietary stress conditions under which the physiological fasting-feeding regulation was impaired. To address this, we generated a conditional SUMO-deficient Prox1 -knock-in mouse model (Prox1_{K556R} K.I. mice). Upon Cre-recombination the genomic region coding for the wild-type variant was removed allowing for the expression of a Prox1 K556R mutant; a schematic representation is shown in Fig 4A. Using an adeno-associated virus (AAV) as a vector to overexpress the Cre recombinase protein under the control of the hepatocyte-specific

LP1 promoter (Cre_AAV), we were able to induce Cre-recombination only in hepatocytes and only after the liver had fully developed. An AAV vector coding for an untranslatable Cre recombinase under the LP1 promoter was used as a control (Ctrl_AAV).

To demonstrate the validity of our model, 8-weeks-old Prox1_{K556R} K.I. male mice were injected with either the Ctrl_AAV, the Cre_AAV, or PBS. The status of Prox1 SUMOylation in the liver was analyzed 3 weeks later. Although the expression of Prox1 at the mRNA and protein levels was constant between the groups, the conjugation of Prox1 with SUMO was abolished in mice injected with the Cre_AAV (Fig 4B). These results confirm that the main SUMOylation event on hepatic Prox1 happens on lysine 556. The hepatocyte-specificity of the Cre recombination driven by the Cre_AAV was confirmed via liver fractionation experiments (Fig EV3A and B).

We then characterized a cohort of male Prox1_{K556R} K.I. mice injected with PBS, Ctrl_AAV or Cre_AAV fed a standard chow diet for 11 weeks. Blood and tissue samples were collected and examined 3–5 h into the dark phase in the fasted and refed states. We identified no differences in terms of body composition, glucose tolerance, insulin sensitivity, lipid metabolism, markers for liver damage, liver weight nor liver morphology (Appendix Figs S1 and S2). In line with the absence of any clear phenotype, the liver transcriptome of control and mice expressing the mutant Prox1 was comparable (Appendix Fig S2E and Dataset EV2). These results suggested that the functionality of the SUMO-switch on Prox1 relies on its

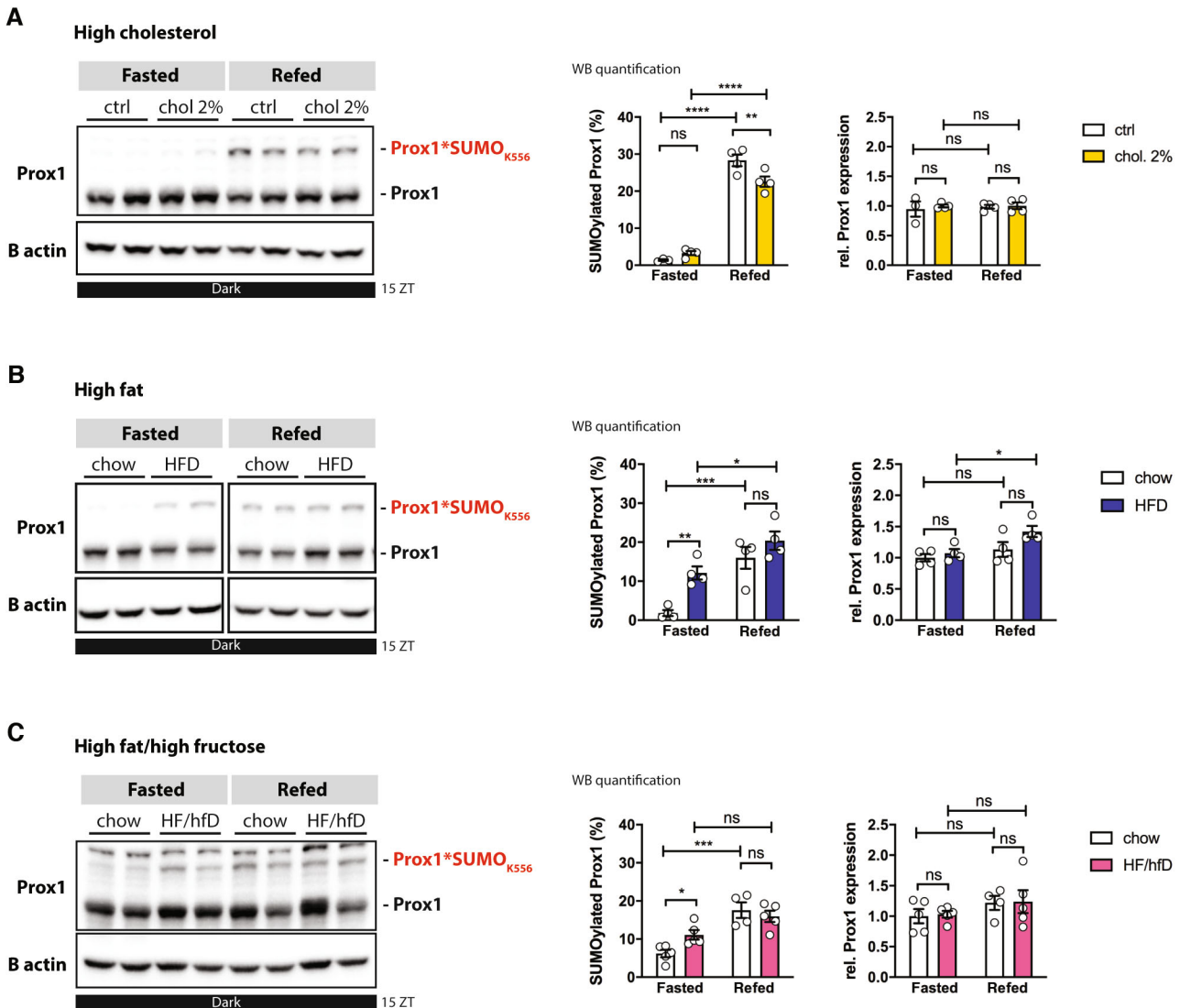


Figure 3. Diet-induced obesity prevents Prox1 de-SUMOylation during fasting.

- A Six-week-old C57BL/6N male mice were fed either a 0% cholesterol diet (ctrl) or a 2% high-cholesterol diet (chol 2%) for 6 weeks.
B Six weeks old C57BL/6N male mice were fed either a standard chow diet or a 60% high fat diet (HFD) for 8 weeks.
C Six-week-old C57BL/6N male mice were fed either a standard chow diet or a 45% high fat +20% w/v fructose diet (HF/hfD) for 1 weeks.
(A–C) Liver samples were collected at ZT 15 in the fasted (11 h) and refed (fasted 8 h and refed 3 h) states ($n = 4\text{--}5$). Liver lysates were analyzed by immunoblotting using anti-Prox1 antibodies; β actin was detected as an input control. The quantification of SUMOylated Prox1 and total Prox1 protein expression are shown.

Data information: Every dot represents one individual mouse. Data: mean \pm SEM. Significance was determined by two-way ANOVA with Sidak's multiple comparison test between different groups and conditions. * $P \leq 0.05$, ** $P \leq 0.01$, *** $P \leq 0.001$, **** $P \leq 0.0001$.

Source data are available online for this figure.

sensitivity to fasting cues and/or becomes relevant only under dietary stress conditions.

To test this idea, we challenged male and female Prox1_{K556R} K.I. mice with a 2% high-cholesterol diet for 14 weeks, a control diet with 0% cholesterol was used as control. Blood and tissue samples were collected and examined 3–5 h into the dark phase in the fasted and refed states. We identified no differences in terms of body composition, glucose tolerance, liver weight nor lipid metabolism (Appendix Figs S3–S5). These results further

support the hypothesis that an impairment of the normal fasting regulation of Prox1 SUMOylation might be necessary to provoke a metabolic phenotype upon genetically altered Prox1 SUMO-deficiency.

Given the altered response of the Prox1 SUMO-switch to fasting cues in a context of diet-induced obesity (Fig 3B and C), we thus next characterized a cohort of male Prox1_{K556R} K.I. mice fed with a 45% high fat +20% w/v fructose diet (HF/hfD) for 18 weeks. Both groups developed an obese phenotype to a

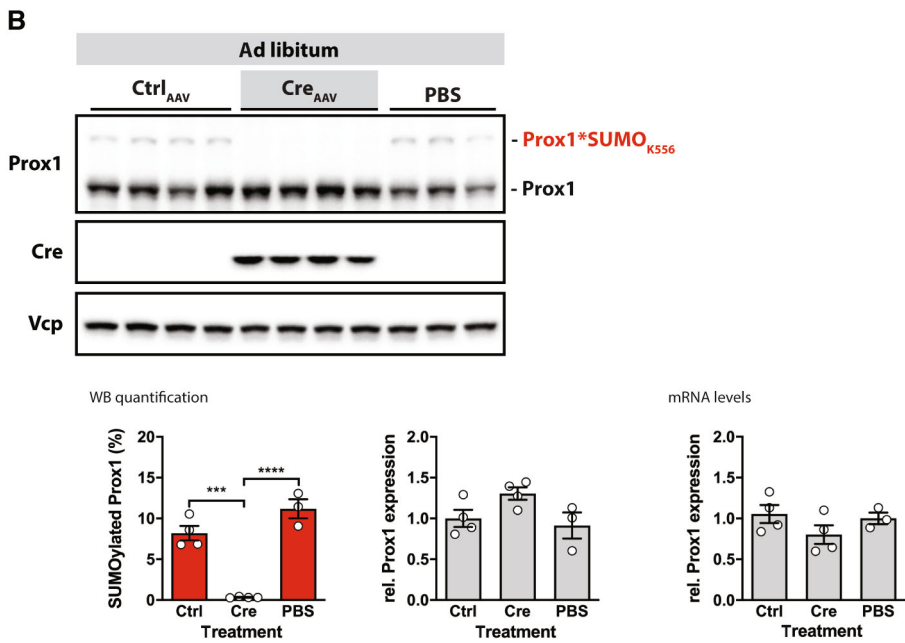
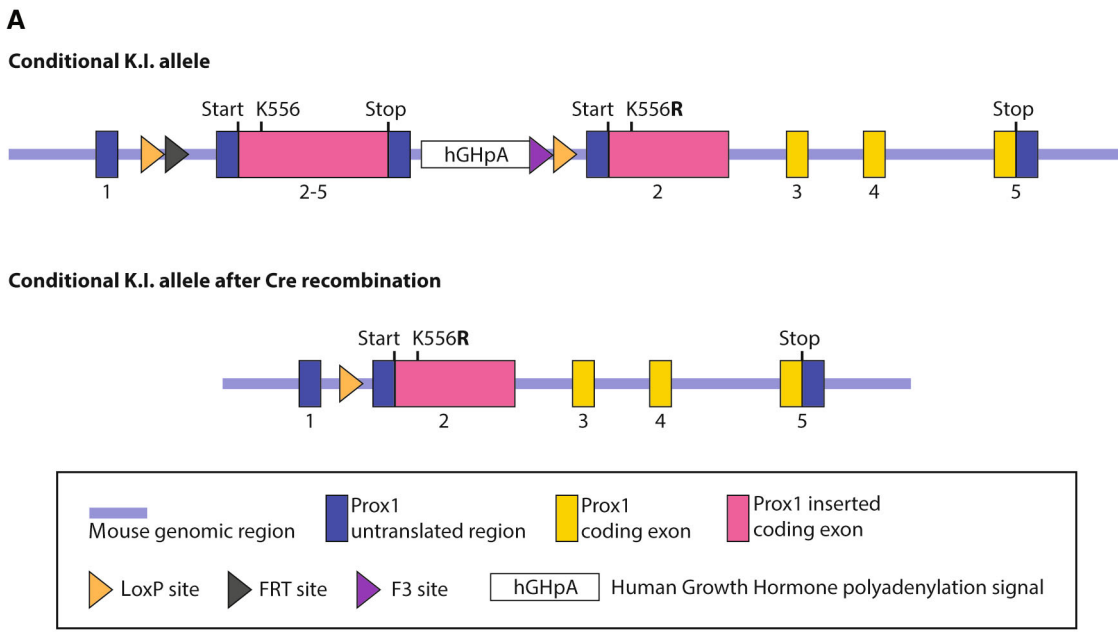


Figure 4. Conditional SUMO-deficient Prox1 knock-in mouse model (Prox1_{K556R} K.I. mice).

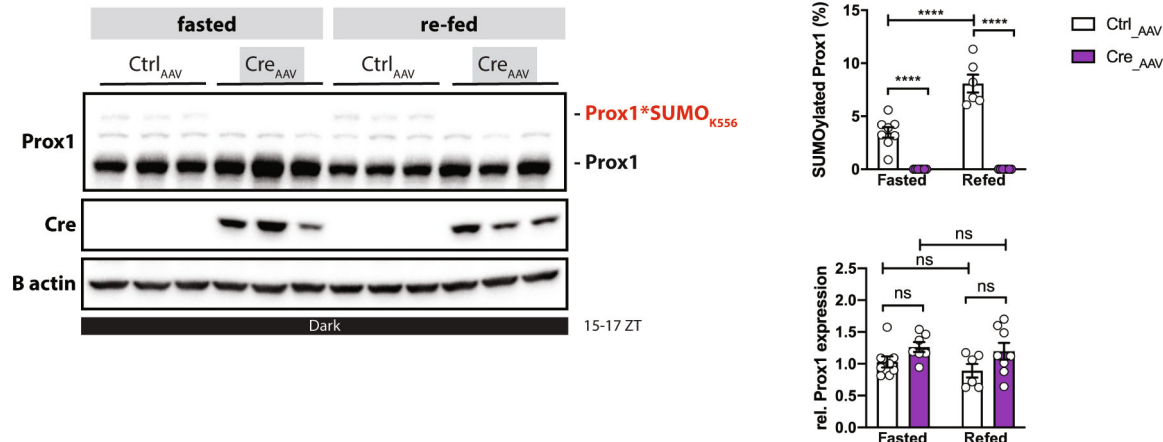
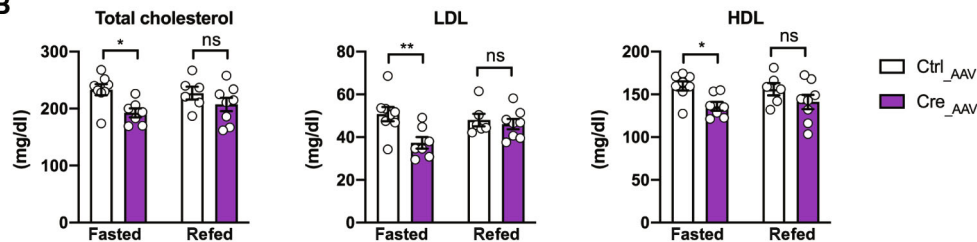
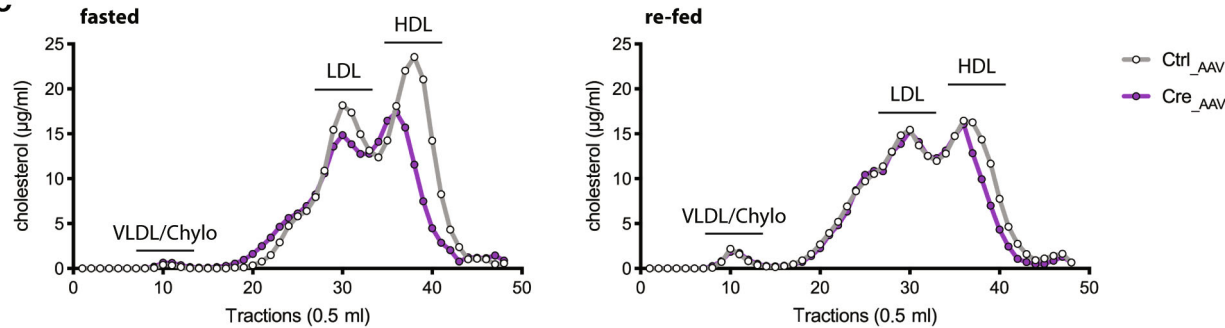
A Schematic representation of the SUMO-deficient Prox1_{K556R} knock-in mouse model.
B 8 weeks old Prox1_{K556R} K.I. (f/f) male mice were injected with a control AAV (Ctrl_AAV), with an AAV to overexpress Cre recombinase (Cre_AAV) or with phosphate-buffered saline (PBS) ($n = 4$). Liver tissue samples were collected 3 weeks later from mice fed ad libitum. Liver lysates were analyzed by immunoblotting using anti-Prox1 and anti-Cre antibodies; Vcp was detected as an input control. The quantification of SUMOylated Prox1 and total Prox1 protein expression as well as Prox1 mRNA levels analyzed by qPCR are shown. qPCR data presented as relative fold change normalized to the housekeeping gene TBP.

Data information: (B) Every dot represents one individual mouse. Data: mean \pm SEM. Significance was determined by one-way ANOVA with Tukey's multiple comparison test between groups. *** $P \leq 0.001$, **** $P \leq 0.0001$.

Source data are available online for this figure.

comparable degree, showing a constant increase in body weight and high fasting blood glucose levels (Fig EV4A). At the end of the study, blood and liver samples were collected and examined

3–5 h into the dark phase in the fasted and refed states. As expected, the conjugation of Prox1 with SUMO was abolished in Prox1_{K556R} K.I. mice injected with the Cre_AAV (Fig 5A). In

A**B****C****Figure 5. Obese mice expressing SUMO-deficient Prox1 in the liver show reduced serum cholesterol.**

A 8 weeks old *Prox1_{K556R}* K.I. (f/f) male mice were injected with a control AAV (Ctrl_AAV) or with an AAV to overexpress Cre recombinase (Cre_AAV) and placed on a high-fat (45%) high-fructose (20% w/v) diet for 18 weeks. Liver samples were collected between ZT 16 and 17 in the fasted (8 h) and re-fed (fasted 8 h and re-fed 4–5 h) states ($n = 7$ –8). Liver lysates were analyzed by immunoblotting using anti-Prox1 and anti-Cre antibodies; β actin was detected as an input control. The quantification of SUMOylated Prox1 and total Prox1 protein expression are shown.

B Serum analysis using a colorimetric-based serum analyzer. Levels of total cholesterol, high-density lipoprotein (HDL) and low-density lipoprotein (LDL) are shown.

C Equal amounts of serum were pooled and separated by FPLC, serum lipoprotein cholesterol profiles are shown.

Data information: (A, B) Every dot represents one individual mouse. Data: mean \pm SEM. Significance was determined by two-way ANOVA with Sidak's multiple comparison test between different groups and conditions. * $P \leq 0.05$, ** $P \leq 0.01$, *** $P \leq 0.0001$.

Source data are available online for this figure.

control animals, the SUMOylated species of Prox1 was detected in both fasted and re-fed states (Fig 5A).

Intriguingly, we identified significantly lower levels of total cholesterol in the circulation of mice expressing the mutant Prox1 as

compared to control mice in the fasted state; the cholesterol reduction was reflected in lower levels of low-density lipoprotein (LDL) and high-density lipoprotein (HDL)-associated cholesterol (Fig 5B). No differences in serum triglycerides or bile acids, nor markers for

liver damage between the control and the mice expressing the mutant Prox1 were identified (Fig EV4B).

To corroborate the cholesterol phenotype, we performed a serum lipoprotein profile by fast protein liquid chromatography (FPLC). In both groups, we measured high levels of LDL and HDL cholesterol as expected from the HF/hfD diet. However, the levels of LDL and HDL associated cholesterol were lower in mice expressing the mutant Prox1 in the fasted state (Fig 5C). Overall, these findings indicate that Prox1 SUMOylation at lysine 556 was specifically responsible for the control of cholesterol handling, while leaving other metabolic parameters intact.

We then analyzed the content of cholesterol within the liver and identified no differences between the control and the mice expressing the mutant Prox1 in terms of total cholesterol or cholesterol esters, which are the storage forms of cholesterol in lipoproteins (Fig EV4C). The liver weight and histological parameters were also comparable between the control and the mice expressing the mutant Prox1 (Fig EV4C and D).

Prox1 SUMOylation on lysine 556 controls the hepatic bile acid detoxification pathway

To investigate how the Prox1 SUMO-switch mediated its impact on cholesterol homeostasis under conditions of diet-induced obesity, we compared the liver transcriptome of mice kept on a HF/hfD diet and expressing either wild-type or SUMO-deficient mutant Prox1 by RNA sequencing. A total of 692 differentially expressed transcripts ($P < 0.05$) were identified in the fasted state, while no transcripts were differentially expressed in the refed state (Fig 6A and Dataset EV3), demonstrating that the single SUMOylation on lysine 556 controls a distinct subset of downstream target genes during fasting.

Functional mapping analysis (KEGG) of the differentially expressed genes in the fasted state revealed an enrichment of pathways involved in retinol metabolism, steroid hormone biosynthesis as well as omega-6 fatty acid metabolism and bile secretion (Fig 6B).

We then examined the function of the individual genes enriched by the pathway analysis and found that most of these genes are involved in the detoxification process of xenobiotics and endogenous molecules such as bile acids and other steroids. The metabolic pathway of detoxification in the liver is driven by enzymes that catalyze the oxidation, reduction, or hydroxylation of toxic molecules (Phase I), conjugation of functional groups such as sulfate and glucuronic acid (Phase II), and export via membrane transporters (Phase III) (Xu *et al*, 2005; Li & Chiang, 2013). The expression of key enzymes mediating Phase I such as cytochrome P450 enzymes (CYPs) and aldehyde dehydrogenases (ALDHs) as well as Phase II such as sulfotransferases (SULTs) and UDP-glucuronosyltransferases (UGTs) were upregulated in the livers of mice expressing the SUMO-deficient Prox1 mutant (Cre_AAV) during fasting (Fig 6C). Furthermore, the predicted gene 5724 coding for the sodium-independent organic anion transport protein (Oatp1a4) and the sodium-dependent bile salt transporter (Slc10a2 also called ASBT) were upregulated in the livers of mice expressing the Prox1 mutant (Fig 6C). The analysis also demonstrated that 3 beta-hydroxysteroid dehydrogenase 5 (Hsd3b5), a steroid reductase, and small heterodimer partner 1 (Shp1 or NR0B2), a key transcriptional regulator of

bile acid synthesis, were downregulated in the liver of mice expressing the Prox1 mutant (Fig 6C).

To test whether these differentially expressed genes were potential direct targets of Prox1, we merged our RNA sequencing data with a published Chip-sequencing analysis on Prox1 (Armour *et al*, 2017). Indeed, Prox1 was enriched at the promoters of key enzymes mediating phase I, II and III of bile acid detoxification as well as factors regulating bile acid synthesis. The occupancy score of the well-described target of Prox1 Cyp7a1 (Qin *et al*, 2004; Ouyang *et al*, 2013) was used as reference (Fig 6C).

These results suggested that obese mice expressing the SUMO-deficient Prox1 mutant had a higher rate of bile acid-mediated cholesterol detoxification during fasting, thus leading to overall reduced cholesterol levels.

There are multiple ways how SUMO conjugation could alter the transcriptional activity of Prox1. We showed via a cycloheximide pulse and chase experiment that SUMOylation did not alter the stability of Prox1 (Fig EV5A). Furthermore, immunofluorescence analysis of HepG2 cells overexpressing wild-type Prox1 or the SUMO-deficient mutants showed that SUMO-conjugation did not affect the nuclear localization of Prox1 (Fig EV5B). We also analyzed the chromatin binding of endogenous Prox1 in salt extraction experiments performed in HepG2 cells and observed that both the unmodified and the SUMOylated species of Prox1 bound strongly to chromatin (Fig EV5C). We then investigated whether SUMO conjugation influenced the interaction of Prox1 with other transcription factors. Prox1 has been shown to interact and repress LRH-1, HNF4 α and PXR, key transcription factors regulating cholesterol and bile acid metabolism (Qin *et al*, 2004; Charest-Marcotte *et al*, 2010; Azuma *et al*, 2011; Dufour *et al*, 2011; Stein *et al*, 2014; Armour *et al*, 2017). We performed co-immunoprecipitation experiments in HEK293A cells overexpressing wild-type (WT) and the SUMO-deficient mutant (KR) together with Myc-tagged LRH-1, HNF4 α and PXR. We observed that the interaction of Prox1 with LRH-1 was much weaker with the KR mutant (Fig 6D), while no differences were detected with HNF4 α or PXR (Fig EV5D). These results suggested that SUMOylation of Prox1 on lysine 556 is required for an optimal interaction with LRH-1, thereby supporting the notion that Prox1 SUMOylation affects distinct interactions with specific transcriptional partner proteins to alter transcriptional responses of downstream target genes.

Taken together, our results establish a nutrition-dependent SUMO-switch on Prox1 in the mouse liver, demonstrating how a single SUMOylation event can exert functional control over hepatic and systemic lipid metabolism.

Discussion

Hepatocytes are specialized cells that are able to sense hormonal cues and orchestrate metabolic programs to maintain energy homeostasis. In this study, we have characterized a nutrient-sensing mechanism in the liver that influences cholesterol metabolism. Prox1, a key transcriptional regulator of lipid metabolism, is modified by SUMOylation on lysine residue 556 in the liver of ad libitum and refed mice but this modification is abolished upon fasting.

Utilizing our conditional SUMO-deficient Prox1_{K556R} K.I. mouse model, we demonstrate that the metabolism of lean mice expressing

the SUMOylation-deficient Prox1 mutant in hepatocytes is comparable to lean mice expressing the wild-type Prox1. However, the response of the SUMO-switch to fasting cues is altered in the liver of

obese mice. Prox1 remains highly modified by SUMOylation even if mice have no access to food. Comparison to mice that carry the mutant form of Prox1 revealed significant transcriptional differences

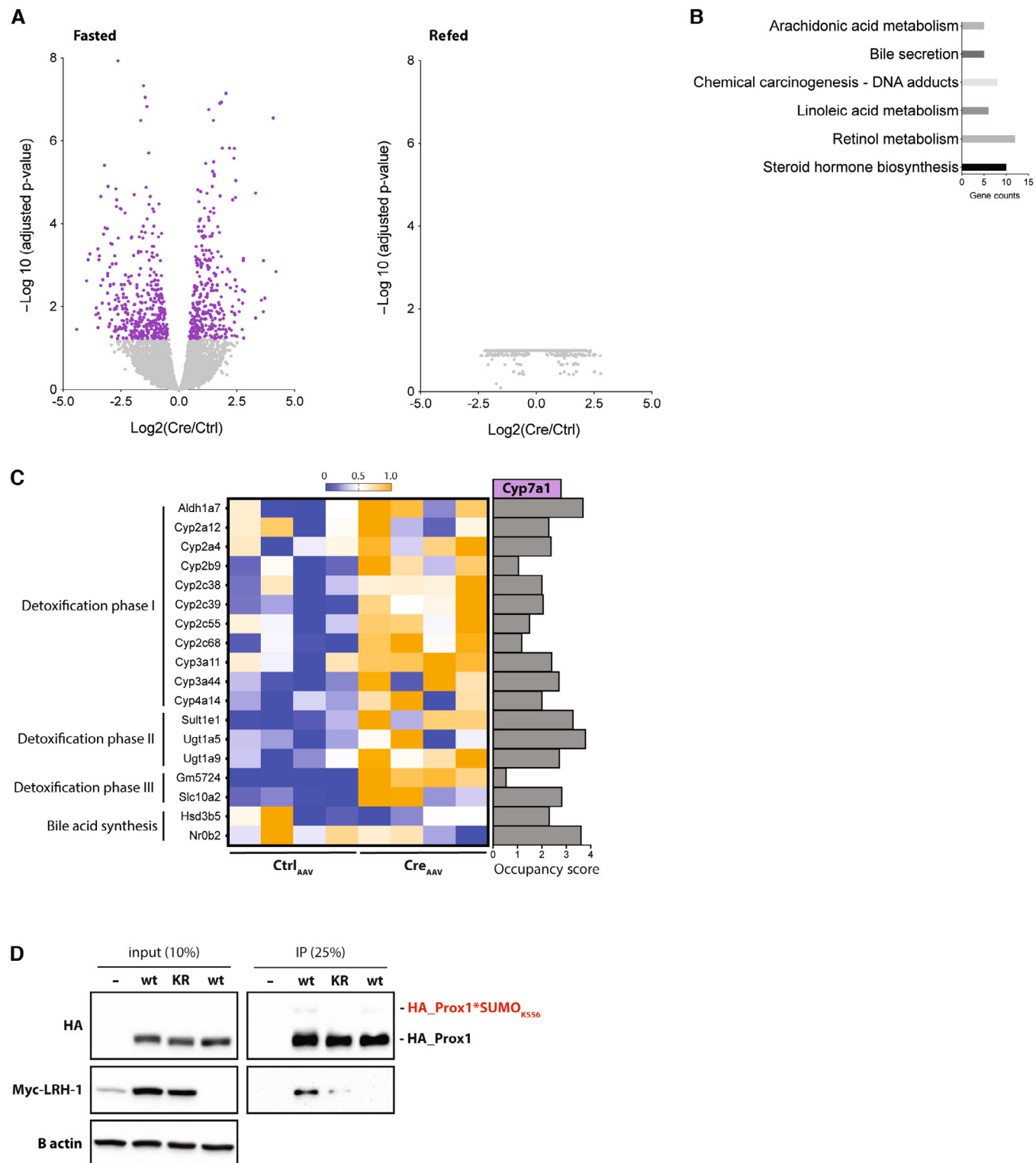


Figure 6.

Figure 6. SUMO-switch on Prox1 controls the hepatic bile acid detoxification pathway.

- A Volcano plots illustrating the genes that are significantly up- or downregulated in the liver of obese mice expressing the Prox1 K556R mutant in comparison to obese mice expressing wild-type Prox1 in the fasted and refed states ($n = 7-8$).
- B Results of a pathway enrichment analysis (KEGG) of the differentially expressed genes in the fasted state.
- C Heatmap displaying the expression of enriched genes involved in phase I, II and III of bile acid detoxification and bile acid synthesis in the liver of obese mice expressing the Prox1 K556R mutant (Cre_AAV) in comparison with obese mice expressing wild-type Prox1 (Ctrl_AAV) in the fasted state ($n = 4$). The occupation scores according to a published Chip- sequencing analysis on Prox1 (Armour et al, 2017) are shown. Cyp7a1 was used as a reference gene.
- D Prox1/LRH-1 co-immunoprecipitation in HEK293A cells overexpressing HA-tagged Prox1 wild-type (wt) or K556R mutant (KR) and Myc-tagged LRH-1.

Source data are available online for this figure.

specifically in the fasted state, and consequently, the “engineered” de-conjugation of Prox1 with SUMO in obese mice has a strong impact on cholesterol metabolism, that is obese mice expressing the SUMO-deficient Prox1 mutant show reduced levels of circulating LDL and HDL cholesterol.

The analysis of the differentially expressed genes in obese mice carrying the SUMO-deficient Prox1 mutant showed higher transcription levels of enzymes and transporters involved the metabolic pathway of bile acid detoxification. Bile acids are synthesized from cholesterol in hepatocytes, conjugated with taurine or glycine, secreted into the bile and stored in the gallbladder. After food ingestion, they are released into the intestine where they are metabolized by intestinal bacteria to produce unconjugated more hydrophobic secondary bile acids that are essential for lipid solubilization and absorption. Around 95% of the bile acids are re-absorbed in the intestinal tract, returned to the liver, and re-secreted into the bile. In addition to their role in lipid absorption, bile acids act as signaling molecules regulating a number of metabolic pathways (Hofmann, 2007; Staels & Fonseca, 2009). However, elevated concentrations of bile acids are cytotoxic. Thus, adaptive responses have evolved to decrease the pool of toxic bile acids. This is achieved by decreasing bile acid synthesis, promoting the metabolism of more hydrophilic bile acids and increasing their elimination (Xie et al, 2001; Xu et al, 2005; Chen et al, 2014).

Obese mice expressing the SUMO-deficient Prox1 mutant show higher transcription levels of Cyp3a11 and Cyp3a44. Enzymes from the Cyp3a family catalyze hydroxylation of bile acids (Honda et al, 2001; Goodwin et al, 2002). Bile acid hydroxylation increases the hydrophilicity of bile acids and thus decreases their toxicity. Hydroxylation of bile acids also facilitates their modification by glucuronidation and sulfation, which increases their solubility and promotes transport and detoxification (Alnouti, 2009; Perreault et al, 2018). Mice expressing the mutant Prox1 show higher levels of the glucuronosyltransferases Ugt1a5 and Ugt1a9 as well as sulfotransferase Sult1e1. In addition, the bile acid transporters Oatp1a4 and Slc10a2 (also called ASBT) are upregulated in mice expressing the mutant Prox1. These transporters are involved in the re-absorption of unconjugated bile acids into hepatocytes for further metabolism and elimination (Lazaridis et al, 1997; Alpini et al, 2001; Xia et al, 2006; van de Steeg et al, 2010). A number of enzymes from the Cyp2c family are also upregulated in mice expressing the mutant Prox1. Enzymes from the Cyp2c cluster catalyze primary bile acids into the more hydrophilic and thus less toxic muricholic acids; this is a process exclusive to the mouse and rat liver (Oteng et al, 2021).

Because cholesterol homeostasis is inherently linked to bile acid metabolism, we propose that higher rates of bile acid detoxification are responsible for the reduced levels of circulating cholesterol in obese mice carrying the SUMO-deficient Prox1 mutant. Indeed, it

has been shown that affecting the composition of the bile acid pool can have significant consequences on cholesterol metabolism. An increase in the recycling of unconjugated hydrophobic bile acids has the potential to enhance the efficiency of bile acid flow and increase bile acid and cholesterol excretion. This process is referred to as the cholehepatic shunt pathway (Hofmann, 1989). An increase in hydrophilic bile acids also reduces cholesterol solubility and absorption in the intestine (Wang et al, 2003). Furthermore, promoting the synthesis pathway for hydrophilic muricholic acids results in lower levels of LDL cholesterol and an increase in fecal cholesterol excretion (Bonde et al, 2016). On the contrary, transgenic mice lacking the Cyp2c cluster and thus lacking muricholic acids have reduced rates of bile acid synthesis and elevated levels of LDL cholesterol (Straniero et al, 2020; Oteng et al, 2021).

But how does SUMO regulate the transcriptional activity of Prox1? Based on published, and our own work, SUMOylation of Prox1 on lysine 556 does neither alter Prox1 stability nor intranuclear localization (Pan et al, 2009) (Fig EV5A and B), but it may affect its ability to bind to the promoter region of specific genes, or may alter its interaction with other transcriptional regulators while bound to DNA. As summarized in recent reviews (Rosonina et al, 2017; Boulanger et al, 2021; Vertegaal, 2022), precedence for either possibility has been observed for other transcription factors.

We believe it is most likely that SUMO conjugation influences the interaction of hepatic Prox1 with other transcription factors and/or transcription coregulators. Indeed, we show in this study that the interaction of Prox1 with LRH-1, a nuclear receptor regulating cholesterol and bile acid metabolism, is promoted by SUMOylation of Prox1. Interestingly, it has been shown that the interaction of Prox1 with LRH-1 is also promoted by SUMOylation of LRH-1 itself (Stein et al, 2014). SUMOylated LRH-1 binds to Prox1 which acts as a co-repressor and inhibits transcription of a select subset of genes controlling hepatic cholesterol uptake and bile flow (Stein et al, 2014). The role of Prox1 SUMOylation mediating protein–protein interactions has also been observed with histone deacetylase 3 (HDAC3), SUMOylation of Prox1 inhibits its interaction with HDAC3 in HEK293 cells (Shan et al, 2008). In the liver, Prox1 has been shown to interact and recruit HDAC3 into the nuclear receptor corepressor (NCoR) complex (Armour et al, 2017).

Therefore, we propose that upon fasting cues, Prox1 is de-SUMOylated to release its repressive activity and promote the transcription of genes involved in bile acid detoxification. This could represent a protective mechanism to avoid toxicity of bile acids that accumulate in the liver and gallbladder when food is not available. This mechanism would become especially relevant under metabolic stress that inflicts pressure on cholesterol metabolism. This hypothesis may explain why the metabolism between lean mice expressing

the SUMO-deficient Prox1 and the lean controls is comparable, while obese mice expressing the SUMO-deficient Prox1 mutant have lower LDL and HDL cholesterol levels compared with the obese controls during fasting.

Together, we have identified a molecular switch in the mouse liver regulated by nutrient availability. In this respect, the SUMO-switch on Prox1 represents an example of SUMOylation as a mechanism to fine-tune transcriptional programs in response to dynamic environmental cues. The maintenance of nutrient-sensitive SUMOylation on Prox1 may thus contribute to the development of “fasting-based” approaches toward improved metabolic health in the future.

Materials and Methods

Generation of AAV_LP1_Cre vectors

A pdsAAV_LP1_GFPmut-miNC plasmid was digested with KpnI and NotI to remove the GFPmut-miNC control sequence. The sequence coding for Cre recombinase was amplified from a bacterial expression construct from St. Jude's Children's Research Hospital, Memphis, TN, USA. Primers were designed to introduce a KpnI restriction site before the Cre recombinase sequence and a NotI restriction site directly after. Parallel amplification reactions were performed to introduce two point mutations and generate two stop codons right after the Kozak sequence. The purified PCR products were ligated into the pdsAAV_LP1 vector. After endotoxin-free plasmid purification, the LP1_Cre_{wt} and LP1_Cre_{mut} sequence integrity and orientation were confirmed by sequencing. To corroborate the integrity of the inverted terminal repeats (ITRs), the plasmids were subjected to a test digestion and the band pattern was controlled by comparison with calculated results. The pdsAAV_LP1_Cre_{wt} and pdsAAV_LP1_Cre_{mut} constructs were used for a large-scale AAV serotype 8 packaging and purification done by Vigene Biosciences Rockville, MD, USA; pDGdelta-helper and p5E18-RC plasmids were provided by our laboratory.

Animal studies

The Prox1_{K556R} K.I. line generated by Taconic Biosciences was back-crossed with wild-type C57BL/6N mice (Charles River) and expanded in the animal facility at Helmholtz Munich Diabetes Center. Eight-week-old Prox1_{K556R} K.I. (f/f) mice were injected with an AAV_LP1_Cre_{wt} (2×10^{11} genome copies) coding for wild-type Cre recombinase to induce the expression of a K556R Prox1 mutant in hepatocytes. An AAV_LP1_Cre_{mut} (2×10^{11} genome copies) coding for an untranslatable Cre mutant was used as a control. The generation of the AAV constructs and the control for hepatocyte specificity is described in detail in the supplemental experimental procedures.

Prox1_{K556R} K.I. and wild-type C57BL/6N mice (Charles River and Janvier laboratories) were maintained on a 12/12 h light/dark cycle and were fed a regular chow diet (Altromin - 1314) ad libitum unless indicated otherwise. For the metabolic challenges, mice were fed either a 0% cholesterol diet (Research Diets—D11112225), a 2% cholesterol diet (Research Diets—D18101201), a 60% high-fat diet (Research Diets—D12492i) or a combination of 45% high-fat diet (Research Diets—D12451i), and 20% w/v fructose (Sigma Aldrich—F0127) water. Animals were randomized by bodyweight prior to

study begin. According to the animal welfare protocol, animals that reached specific exclusion criteria regarding food intake, body weight, and overall health were excluded from the study.

Fasting and refeeding schedules are explained in the main text and in the figure legends; Zeitgeber (ZT) 0 = lights on and ZT 12 = lights off.

All animal studies were performed in accordance with German animal welfare legislation and in specific pathogen-free conditions in the animal facility of the Helmholtz Center, Munich, Germany. Protocols were approved by the institutional animal welfare officer, and necessary licenses were obtained from the state ethics committee and government of Upper Bavaria (ROB-55.2-2532.Vet_02-17-49, ROB-55.2-2532.Vet_02-15-164 and ROB-55.2-2532.Vet_02-21-66).

Control of Cre recombination specificity by liver fractionation

Eight-week-old Prox1K556R K.I. (f/f) mice were injected with either the AAV_LP1_Cre_{wt} or the AAV_LP1_Cre_{mut} (2×10^{11} genome copies). Three weeks later, the hepatocyte cell fraction was separated from the nonhepatocyte fraction following the protocol generated by (Godoy *et al*, 2013). In brief: Mice were anesthetized, both abdominal walls were opened, and the liver was perfused through the venae cavae with a warm EGTA-containing KH/HEPES buffer for 10 min. The liver was then perfused with a warm collagenase-KH/HEPES buffer for 12 min until liver digestion was visible. The perfused liver was then removed, incubated in suspension buffer (KH/HEPES containing 400 mg BSA) and dissociated by gentle shaking. The cell suspension was filtered through a 100 nm pore mesh and centrifuged at 50 g for 5 min at 4°C. The pellet containing the hepatocyte fraction was washed two times with suspension buffer and centrifuged at 50 g for 5 min at 4°C. The supernatant containing the nonhepatocyte fraction was transferred to a clean container and cleared by a second centrifugation round at 50 g for 5 min at 4°C. The clean supernatant was then centrifuged at 800 g for 10 min to pellet the nonhepatocyte cell fraction. The liver fractionation was controlled by detecting the expression of albumin, an hepatocyte-specific marker, as well as Stab1, Emr1 and Vim, which are markers of sinusoidal endothelial cells, kupffer cells, and hepatic stellate cells, respectively.

A PCR was then performed using primers designed by Taconic Biosciences to detect either the constitutive allele or the conditional knock-in (K.I.) allele after Cre-mediated recombination.

Amplification with these primers gives a product of 280 bp for the constitutive allele and a 235 bp product for the conditional K.I. allele.

In vivo characterization protocols

Glucose and Insulin tolerance tests: For the glucose tolerance test (GTT), mice were fasted for 5–6 h (ZT 2–8) then challenged with 1.5 g/kg glucose via an intraperitoneal injection. Blood samples were collected in heparin-coated tubes at time points: 0 and 15 min from the tail vein; the blood glucose levels were recorded with a glucometer at time points: 0, 15, 30, 60, and 120 min. Blood samples were centrifuged at 2,000 g for 5 min at 4°C; the plasma was collected, snap-frozen in liquid nitrogen, and stored at –80°C. The plasma insulin content was measured with a mouse insulin ELISA (ALPCO—80-INSMS-E10). For the insulin tolerance test (ITT), mice

were fasted for 5 h (ZT 2-7) then challenged with 1.2 U/kg insulin via an intraperitoneal injection. Blood glucose levels were recorded with a glucometer at time points: 0, 15, 30, 60, and 120 min from the tail vein.

Blood sampling: Blood samples of 20–60 µl volume were collected in heparin-coated tubes by piercing the tail vein. Blood samples were centrifuged at 2,000 g for 5 min at 4°C; the plasma was collected, snap-frozen in liquid nitrogen, and stored at –80°C.

Tissue collection, serum analysis, and lipoprotein profile by fast protein liquid chromatography

Body weight and blood glucose levels were recorded in every study prior to tissue collection. Mice were sacrificed by cervical dislocation and decapitated immediately. Blood was collected in serum gel tubes, incubated at room temperature for 5–10 min, and stored at 4°C until further processing. The collection of liver samples from wild-type mice was done using prefrozen forceps, and all samples were collected from the left lobe. For the characterization of Prox1_{K556R} K.I. mice, the tissues were collected, weighed, washed in PBS, and snap-frozen in liquid nitrogen. A sample from the medial liver lobe was placed in a histocasette and incubated in formalin for fixation. Once all tissues were collected, the blood samples were centrifuged at 2,000 g for 10 min at 4°C; the serum was collected and snap-frozen in liquid nitrogen. Tissue and serum samples were stored at –80°C.

Individual serum samples were analyzed using an automatized system (Beckman Coulter AU480 Chemistry Analyzer).

To generate a lipoprotein profile, serum samples were pooled and subjected to gel filtration by fast protein liquid chromatography using a Superose 6 10/300 GL column (Cytiva 17-5172-01). The cholesterol content of individual fractions was determined using a total cholesterol assay kit (Invitrogen A12216).

Histology

Tissue samples were harvested and immediately fixed with neutrally buffered formalin (4% w/v) (Sigma Aldrich—Aldrich—HT501128) and subsequently routinely embedded in paraffin (Tissue Tec VIP.6 Sakura Europe). Sections of 3 µm were stained with hematoxylin and eosin (HE) and with Sirius red, using a HistoCore SPECTRA ST automated slide stainer (Leica) with prefabricated staining reagents according to the manufacturer's instructions. The stained tissue sections were scanned with an AxioScan.Z1 digital slide scanner (Zeiss) equipped with a 20× magnification objective. Quantification of the lipid amount was morphometrically determined on H&E-stained liver sections.

Liver glycogen, triglycerides and cholesterol measurements

For glycogen measurements: Liver tissue pieces were weighted (45–55 mg) and homogenized in 0.5 ml of a KOH (30%) solution. Samples were mixed at 1,000 rpm for 1 h at 95°C then centrifuged at 500 g for 5 min at room temperature. The supernatant was collected and mixed with 1.4 ml ice-cold ethanol (95%), incubated for 30 min at –20°C and centrifuged at 3,000 g for 20 min at room temperature. The pellets were washed with ethanol (95%), dried for 10 min at 60°C, and dissolved in 0.25 ml distilled water at 37°C.

Glycogen content was measured using a glycogen assay kit (Sigma Aldrich—Aldrich) according to the manufacturer's protocol.

For lipid measurements: Liver tissue pieces were weighted (60–80 mg) and homogenized in 1.5 ml of a chloroform:methanol (2:1) solution. Samples were mixed at 1,400 rpm for 20 min at room temperature then centrifuged at 15,500 g for 30 min at room temperature. The liquid phase was collected and mixed with 0.2 ml NaCl (150 mM) and centrifuged at 370 g for 5 min. 0.2 ml of the organic phase was mixed with 40 µl of a chloroform:Triton-X (1:1) solution and dried overnight with the speed-vac V-AL program in the Concentrate plus (Eppendorf). The Triton-X lipid solution was diluted (1.125×) in 0.2 ml of distilled water by mixing (end-to-end rotation) for 1 h at room temperature. Triglycerides were measured using a Triglycerides determination kit (Sigma Aldrich—Aldrich) according to the manufacturer's protocol using 2 µl of lipid solution. Cholesterol levels were measured using a total cholesterol assay kit (Cell Biolabs Inc.) according to the manufacturer's protocol using 2 µl of lipid solution.

Lysate preparation and immunoblot analysis

Around 20 mg of frozen liver tissue was lysed and homogenized using a tissue lyser (Retsch—MM400) with steel beads in 500 µl ice-cold lysis buffer containing Tris (50 mM) pH 6.8, EDTA (1 mM), NaCl (150 mM), Igepal (1%), and N-Ethylmaleimide (10 mM) as isopeptidase inhibitor (Sigma Aldrich—E3876) supplemented with protease and phosphatase inhibitors in tablets (Roche - 42484600 and 4906845001, respectively). The lysates were incubated on a rotator wheel for 30 min at 4°C, sonicated at a 20% amplitude for 5 pulses (1 s pulse and 1 s break) and centrifuged at 18,000 g for 30 min at 4°C. Cell lysates were prepared following the same protocol. Protein lysates were analyzed by immunoblotting using anti-Prox1 (Millipore —07-537 and Abcam—ab38692), anti-Phospho_S6K_(Thr389) (Cell Signaling—9234), anti-Cre Recombinase (Cell Signaling—15036), goat anti-RanGAP1 (produced by our collaborator at the Melchior lab), anti-β actin (Sigma Aldrich—A5441), anti-Vcp (Abcam—ab11433), anti-HA tag (Cell Signaling—2367), anti-tubulin (Santa Cruz—5274) and anti-RCC1 (BD Biosciences—610377) antibodies. Blots were analyzed and quantified with Image Lab (Bio-Rad Laboratories).

Liquid chromatography (LC)-coupled mass spectrometry (MS) of immuno-purified proteins

SUMO immunoprecipitation from liver tissue samples was performed as described (Becker *et al.*, 2013; Barysch *et al.*, 2014). Eluted proteins from control immunoprecipitation, SUMO1 immunoprecipitation and SUMO2 immunoprecipitation each derived from fasted (16 h) and refed (fasted 16 h and re-fed 2 h) mice were separated with 1D SDS-PAGE. Each lane was cut into equal pieces before undergoing in-gel digestion of proteins in each gel slide with trypsin overnight. Eluted peptides were dried in a SpeedVac concentrator and dissolved for further processing as described previously (Becker *et al.*, 2013). LC-MS/MS analyses were made as described previously (Becker *et al.*, 2013). Database search of MS data was performed with Mascot (matrixscience.com) against the NCBI nonredundant database of *Mus. musculus* (24.02.2011, 471,874 entries). For databases search, two missed cleavages were allowed, methionine oxidation and carbamidomethyl at cysteine were set as

variable modifications. The precursor tolerance was set to 10 ppm and the fragment tolerance to 0.6 Da. Data were visualized with the Scaffold software (Proteomesoftware.com), and proteins identified in the different samples were ranked according to their total spectrum count.

Gene expression analysis

Around 5 mg of liver tissue were homogenized using a tissue lyser (Retsch—MM400) with steel beads in 1 ml Trizol (Thermo Scientific—15596018). The samples were mixed with 0.2 ml chloroform, the aqueous phase was collected and mixed with 0.6× volumes of 100% ethanol. The samples were loaded on an EconoSpin column, and the RNA was washed three times with RPE buffer (QIAGEN). The RNA was eluted with distilled nuclease free water. The RNA concentration was determined with a NanoDrop 2000 spectrophotometer (Thermo Scientific) and the integrity was controlled by gel electrophoresis using an RNA 6000 Nano Kit (Agilent) according to the manufacturer's protocol using a 2100 Bioanalyzer (Agilent). RNA samples were diluted to a 100 ng/μl concentration and stored at –80°C.

For the qPCR expression analysis, cDNA was generated from 1 μg of RNA with the QuantiTect Reverse Transcription Kit (QIAGEN) according to the manufacturer's protocol. The expression of selected genes was analyzed using the TaqMan Gene Expression reagents (Thermo Scientific) with the QuantStudio 6 Flex Real-Time PCR system (Thermo Scientific).

The RNA sequencing libraries were generated by the sequencing facility of the Helmholtz Center Munich (chow study) or by Novogene Europe (Hf/hf study). The adapter sequence from the raw files was removed by using Cutadapt 4.1. Raw counts were then aligned to the mouse reference genome using STAR 2.7.10a. Any genes that have no transcript detected in any samples were removed. Data normalization and differential expression analysis were performed using the DESeq2 R-package from Bioconductor (Love *et al*, 2014). A statistical threshold was set to an adjusted *P*-value (*Padj*) < 0.05; DESeq2 uses the Benjamini–Hochberg to adjust for multiple testing. A threshold for the effect size was set to a log₂ fold change (FC) of < –0.5 or >0.5. Analysis of the differentially expressed genes for biological pathways was performed using the enrichKEGG function (Kyoto Encyclopedia of Genes and Genomes database).

Generation of HA-Prox1 and YFP-Prox1 constructs

Prox1-specific primers were designed to amplify the sequence coding for Prox1 from mouse cDNA. A BamHI restriction site was introduced directly before the translation start site, and an EcoRI restriction site was introduced directly after the translation termination site. The purified PCR product was ligated into a pcDNA3 vector containing an N-terminal HA tag (Invitrogen). The Prox1 K556R and E558A mutants were generated by site-directed mutagenesis using the QuikChange Site-Directed Mutagenesis Kit according to the manufacturer's protocol (Agilent). The sequence integrity and orientation were confirmed by sequencing.

The sequences coding for Prox1 wild-type and mutants were cloned from the pcDNA3 into a pEYFP-C1 vector. Primers were designed to introduce a SalI restriction site followed by a PreScission protease recognition site directly before the translation

start site, XbaI restriction site was introduced directly after the translation termination site. The sequence integrity and orientation were confirmed by sequencing.

Purification of full-length mouse Prox1

YFP-Prox1 was transfected into HEK293T cells (Thermo Fischer Scientific) with polyethylenimine for 48 h. The cells were collected with ice-cold PBS and centrifuged at 1,000 g for 5 min at 4°C, the cell pellet was washed one more time with ice-cold PBS. Cells were then lysed with 1 ml of ice-cold assay buffer containing Tris (50 mM) pH 7.5, EDTA (5 mM), EGTA (5 mM), NaCl (150 mM), Igepal (0.5%) supplemented with protease inhibitors. Cell lysates were sonicated at a 20% amplitude for 15 pulses (1 s pulse and 1 s break), incubated on ice for 30 min then clarified by centrifugation at 20,000 g for 30 min at 4°C. GFP-binder beads pre-equilibrated in assay buffer were incubated with the lysates (around 5 μl GFP-binder beads per 1 mg protein) overnight with a constant agitation at 4°C. The GFP-binder beads were collected by centrifugation at 800 g for 5 min at 4°C using a swing-out rotor. The beads were washed twice with 1 ml of ice-cold RIPA buffer and three times more with 1 ml of ice-cold assay buffer supplemented with DTT (1 mM). During the last wash, the beads were transferred into a 0.5-ml tube in 300 μl of assay buffer supplemented with DTT (1 mM) and 2 μg GST-tagged PreScission protease. The cleavage was performed for 4 h with a constant agitation at 4°C. The GFP-beads were collected by centrifugation at 800 g for 5 min at 4°C using a swing-out rotor and the supernatant was transferred to a fresh 0.5-ml tube. To remove the GST-tagged PreScission protease, the eluate was incubated with 10 μl GST-binder beads pre-equilibrated in assay buffer supplemented with DTT (1 mM) for 1.5 h with a constant agitation at 4°C. The GST-binder beads were collected by centrifugation at 500 g for 5 min at 4°C using a swing-out rotor and the eluate was concentrated to a volume of 50–100 μl using a VIVASPIN 0.5 ml centrifugal concentrator (Millipore) according to the manufacturer's instructions. The eluate was snap-frozen in liquid nitrogen and stored at –80°C.

In vitro SUMOylation assay

In vitro SUMOylation reactions were made with purified mouse wild-type or K556R Prox1 (100 nM) together with recombinant E1 Aos1/Uba2 (100 nM) and E2 Ubc9 (200 nM) in the presence of either SUMO1 or SUMO2 (5 μM). The reactions were carried out in a volume of 20 μl assay buffer: HEPES/KOH (20 mM) pH 7.3, KAcO (110 mM), Mg (AcO)₂ (2 mM), EGTA (1 mM), DTT (1 mM) and Tween 20 (0.05% v/v) supplemented with protease inhibitors and ovalbumin (0.2 mg/ml) at 30°C. The reactions were initiated by adding ATP (1 mM) and stopped by the addition of 20 μl 2× SDS sample buffer. Purification of mouse Prox1 is described in detail in the supplemental experimental procedures. Recombinant E1, E2, and SUMO proteins were purified as described (Pichler *et al*, 2004; Werner *et al*, 2009).

Co-immunoprecipitation

HEK293A cells (Thermo Fischer Scientific—R70507) were transfected with mouse HA-tagged wild-type Prox1 (wt) or K556R mutant

together with mouse Myc-tagged HNF4 α (Origene—MR227662), Myc-tagged LRH-1 (Origene—MR225371) or Myc-tagged PXR (Origene—MR226044) using Lipofectamine 3000 with Plus Reagent (Thermo Fisher Scientific) according to the manufacturer's protocol. Forty-eight hours later, the cells were lysed with ice-cold lysis buffer containing Tris (50 mM) pH 8, EDTA (0.5 mM), NaCl (150 mM), Igepal (0.25%), glycerol (2.5%), and N-Ethylmaleimide (10 mM) as isopeptidase inhibitor (Sigma Aldrich—E3876) supplemented with protease and phosphatase inhibitors in tablets (Roche - 42484600 and 4906845001, respectively). Cells were lysed by freezing in liquid nitrogen and thawing, and incubated on a rotator wheel for 15 min at 4°C. Finally, the lysates were centrifuged at 10,000 g for 15 min at 4°C. Equal amounts of total protein (around 400 µg) were diluted 1:1 with ice-cold IP-buffer containing HEPES (20 mM) pH 8, KCl (75 mM), MgCl₂ (2.5 mM) and N-Ethylmaleimide (10 mM) as isopeptidase inhibitor (Sigma Aldrich - E3876) supplemented with protease and phosphatase inhibitors in tablets (Roche - 42484600 and 4906845001 respectively). Protein samples were then incubated with 25 µl anti-HA Magnetic Beads (Thermo Fisher Scientific—88836) on a rotator wheel at 4°C over night. The beads were then washed twice with IP-buffer and once with wash buffer containing HEPES (20 mM) pH 8, KCl (75 mM), MgCl₂ (2.5 mM), Tween-20 (0.1%), and N-Ethylmaleimide (10 mM) as isopeptidase inhibitor (Sigma Aldrich—E3876) supplemented with protease and phosphatase inhibitors in tablets (Roche—42484600 and 4906845001 respectively). Bound proteins were eluted with 60 µl Laemmli SDS sample buffer (1×) by incubating 5 min at 95°C.

Immunofluorescence microscopy

HepG2 cells (ATTC—HB/8065) were transfected with mouse YFP-tagged wild-type Prox1 (wt) or K556R mutant Prox1 using Lipofectamine 3000 with Plus Reagent (Thermo Fisher Scientific) according to the manufacturer's protocol. Forty-eight hours later, the cells were fixed in PFA for 15 min at room temperature. Cells were washed with PBS and permeabilized with Triton X-100 (0.1%) in PBS for 10 min. Cells were stained with DAPI and mounted on glass slides with Mowiol 4-88 (0.1 g/ml). Samples were analyzed using a laser scanning confocal microscope (Olympus Fluoview 1200, Olympus Corporation) equipped with Olympus UPlanSAPO ×60 1.35 and UPlanSAPO ×40 1.25 oil immersion objectives (Olympus Corporation).

Cycloheximide pulse and chase assay

HEK293A cells (Thermo Fischer Scientific—R70507) were transfected with mouse HA-tagged wild-type Prox1 (wt), K556R or E558A mutant using Lipofectamine 3000 with Plus Reagent (Thermo Fisher Scientific) according to the manufacturer's protocol. Forty-eight hours later, the cells were treated with 100 µg/ml cycloheximide for 6 and 8 h. Cell lysates were prepared and analyzed as described above.

Salt-gradient endogenous Prox1 extraction from HepG2 cell nuclei

Cells were washed twice with ice-cold PBS by centrifugation at 1,000 g for 5 min at 4°C. Cells were then incubated for 3 min with

5× pellet volume ice-cold cytoplasmic buffer containing HEPES (10 mM), EDTA (1 mM), EGTA (1 mM), KCl (60 mM), Igepal (0.075%) supplemented with protease and phosphatase inhibitors (pH = 7.6). Cell lysis was controlled by trypan blue staining (up to 70–80% cell lysis). The sample was then centrifuged at 1,500 g for 4 min at 4°C and the cytoplasmic extract was transferred to a fresh tube. The nuclear pellet was gently washed with 3× pellet volume ice-cold cytoplasmic buffer by pipetting up and down and centrifuged at 1,500 g for 4 min at 4°C. The nuclear pellet was then incubated for 10 min with 2× pellet volume ice-cold nuclear buffer containing HEPES (20 mM), MgCl₂ (1.5 mM), EGTA (0.2 mM), glycerol (25%) supplemented with protease and phosphatase inhibitors (pH = 7.9). Parallel extractions were made using the nuclear buffer supplemented with different NaCl concentrations (110, 230, 350 or 420 mM). Samples were vortexed periodically to re-suspend the pellet. Finally, the nuclear extracts were centrifuged at 1,500 g for 4 min at 4°C and transferred to a fresh tube. The cytoplasmic and nuclear extracts were clarified by centrifugation at 20,000 g for 30 min at 4°C. Samples were snap-frozen in liquid nitrogen and stored at –80°C.

Statistical analyses

Data expressed as means ± SEM. Comparison of time-course experiments was assessed by one-way ANOVA with Dunnett's multiple comparison test relative to samples collected at ZT 12. Multiple group comparisons were assessed by one-way ANOVA with Tukey's multiple comparison test between groups. Multiple group comparisons of two factors (fasted and refed) were assessed by two-way ANOVA with Sidak's multiple comparison test between different groups and conditions.

$P \leq 0.05$ was considered statistically significant. * $P \leq 0.05$, ** $P \leq 0.01$, *** $P \leq 0.001$, **** $P \leq 0.0001$.

Data availability

The mass spectrometry proteomics data have been deposited to the ProteomeXchange Consortium via the PRIDE (Perez-Riverol *et al*, 2022) partner repository with the dataset identifier PXD041329 (<http://proteomecentral.proteomexchange.org/cgi/GetDataset?ID=PXD041329>). The RNA sequencing data have been deposited to the Gene Expression Omnibus depository under the GEO accession codes GSE237590 (<https://www.ncbi.nlm.nih.gov/geo/query/acc.cgi?acc=GSE237590>); GSE237593 (<https://www.ncbi.nlm.nih.gov/geo/query/acc.cgi?acc=GSE237593>).

Expanded View for this article is available [online](#).

Acknowledgments

We would like to thank Andrea Takas, Elena Vogl, Jeanette Biebl, Daniela Hass, and Sebastian Cucuruz for their technical expertise. We thank Luke Harrison for proof reading and editorial support. The graphical abstract and part of Fig 1 were created with [Biorender.com](#). The work of the authors is supported by the German Research Foundation (DeutscheForschungsgemeinschaft, DFG) within the CRC/Transregio 205/2, Project number: 314061271 – TRR 205 “The Adrenal: Central Relay in Health and Disease” to Stephan Herzig, the SFB1321 (Project-ID 329628492 to Stephan Herzig), and the SFB1118 (Project A01 to

Stephan Herzig); Helmholtz Future Topic Aging and Metabolic Programming (AMPro, ZT-0026) to Stephan Herzig; Else-Kröner-Fresenius-Stiftung (2020 EKSE.23 to Stephan Herzig) and the Edith–Haberland–Wagner Stiftung to Stephan Her and the DKFZ-ZMBH Alliance to Frauke Melchior and Claudia Dittner. Open Access funding enabled and organized by Projekt DEAL.

Author contributions

Ana Jimena Alfaro: Data curation; software; formal analysis; validation; investigation; visualization; methodology; writing – original draft; writing – review and editing. **Claudia Dittner:** Data curation; formal analysis; investigation; methodology. **Janina Becker:** Data curation; formal analysis; investigation; methodology. **Anne Loft:** Data curation; methodology. **Amit Mhamane:** Data curation; software; formal analysis; visualization; methodology. **Adriano Maida:** Methodology; project administration. **Anastasia Georgiadi:** Methodology. **Foivos-Filippou Tsokanos:** Methodology. **Katarina Klepac:** Methodology. **Claudia-Eveline Molocea:** Methodology. **Rabih El-Merahbi:** Methodology. **Karsten Motzler:** Methodology. **Julia Geppert:** Methodology. **Rhoda Karikari:** Methodology. **Julia Szendrődi:** Conceptualization. **Annette Feuchtinger:** Methodology. **Susanna Hofmann:** Methodology. **Samir Karaca:** Data curation; formal analysis; validation; methodology. **Henning Urlaub:** Resources; data curation; validation; methodology. **Mauricio Berriel Diaz:** Formal analysis; supervision; investigation; methodology. **Frauke Melchior:** Conceptualization; writing – review and editing. **Stephan Herzig:** Conceptualization; resources; supervision; funding acquisition; writing – original draft; project administration; writing – review and editing.

Disclosure and competing interests statement

The authors declare that they have no conflict of interest.

References

- Alegre KO, Reverter D (2011) Swapping small ubiquitin-like modifier (SUMO) isoform specificity of SUMO proteases SENP6 and SENP7. *J Biol Chem* 286: 36142–36151
- Alnouti Y (2009) Bile acid sulfation: a pathway of bile acid elimination and detoxification. *Toxicol Sci* 108: 225–246
- Alpini G, Ueno Y, Glaser SS, Marzoni M, Phinizy JL, Francis H, Lesage G (2001) Bile acid feeding increased proliferative activity and apical bile acid transporter expression in both small and large rat cholangiocytes. *Hepatology* 34: 868–876
- Armour SM, Remsberg JR, Damle M, Sidoli S, Ho WY, Li Z, Garcia BA, Lazar MA (2017) An HDAC3-PROX1 corepressor module acts on HNF4α to control hepatic triglycerides. *Nat Commun* 8: 549
- Azuma K, Urano T, Watabe T, Ouchi Y, Inoue S (2011) PROX1 suppresses vitamin K-induced transcriptional activity of Steroid and Xenobiotic Receptor. *Genes Cells* 16: 1063–1070
- Balasubramanyan N, Luo Y, Sun A-Q, Suchy FJ (2013) SUMOylation of the Farnesoid X Receptor (FXR) Regulates the expression of FXR target genes. *J Biol Chem* 288: 13850–13862
- Banerjee P, Kumaravel S, Roy S, Gaddam N, Odeh J, Bayless KJ, Glaser S, Chakraborty S (2023) Conjugated bile acids promote lymphangiogenesis by modulation of the reactive oxygen species-p90RSK-vascular endothelial growth factor receptor 3 pathway. *Cells* 12: 526
- Barysch SV, Dittner C, Flotho A, Becker J, Melchior F (2014) Identification and analysis of endogenous SUMO1 and SUMO2/3 targets in mammalian cells and tissues using monoclonal antibodies. *Nat Protoc* 9: 896–909
- Bechmann LP, Hannivoort RA, Gerken G, Hotamisligil GS, Trauner M, Canbay A (2012) The interaction of hepatic lipid and glucose metabolism in liver diseases. *J Hepatol* 56: 952–964
- Becker J, Barysch SV, Karaca S, Dittner C, Hsiao HH, Berriel Diaz M, Herzig S, Urlaub H, Melchior F (2013) Detecting endogenous SUMO targets in mammalian cells and tissues. *Nat Struct Mol Biol* 20: 525–531
- Bonde Y, Eggertsen G, Rudling M (2016) Mice abundant in muricholic bile acids show resistance to dietary induced steatosis, weight gain, and to impaired glucose metabolism. *PLoS One* 11: e0147772
- Boulanger M, Chakraborty M, Tempé D, Piechaczyk M, Bossis G (2021) SUMO and transcriptional regulation: the lessons of large-scale proteomic, modifomic and genomic studies. *Molecules* 26: 828
- Burke Z, Oliver G (2002) Prox1 is an early specific marker for the developing liver and pancreas in the mammalian foregut endoderm. *Mech Dev* 118: 147–155
- Chang C-C, Naik Mandar T, Huang Y-S, Jeng J-C, Liao P-H, Kuo H-Y, Ho C-C, Hsieh Y-L, Lin C-H, Huang N-J et al (2011) Structural and functional roles of Daxx SIM phosphorylation in SUMO paralog-selective binding and apoptosis modulation. *Mol Cell* 42: 62–74
- Charest-Marcotte A, Dufour CR, Wilson BJ, Tremblay AM, Eichner LJ, Arlow DH, Mootha VK, Giguère V (2010) The homeobox protein Prox1 is a negative modulator of ERR α /PGC-1 α bioenergetic functions. *Genes Dev* 24: 537–542
- Chen J, Zhao KN, Chen C (2014) The role of CYP3A4 in the biotransformation of bile acids and therapeutic implication for cholestasis. *Ann Transl Med* 2: 7
- Di Bacco A, Ouyang J, Lee H-Y, Catic A, Ploegh H, Gill G (2006) The SUMO-specific protease SENP5 is required for cell division. *Mol Cell Biol* 26: 4489–4498
- Dudas J, Papoutsi M, Hecht M, Elmaouhoub A, Saile B, Christ B, Tomarev SI, von Kaisenberg CS, Schweigerer L, Ramadori G et al (2004) The homeobox transcription factor Prox1 is highly conserved in embryonic hepatoblasts and in adult and transformed hepatocytes, but is absent from bile duct epithelium. *Anat Embryol* 208: 359–366
- Dufour CR, Levasseur M-P, Pham NHH, Eichner LJ, Wilson BJ, Charest-Marcotte A, Duguay D, Poirier-Héon J-F, Cermakian N, Giguère V (2011) Genomic convergence among ERR α , PROX1, and BMAL1 in the control of metabolic clock outputs. *PLoS Genet* 7: e1002143
- Elsir T, Smits A, Lindström MS, Nistér M (2012) Transcription factor PROX1: its role in development and cancer. *Cancer Metastasis Rev* 31: 793–805
- Flotho A, Melchior F (2013) Sumoylation: a regulatory protein modification in health and disease. *Annu Rev Biochem* 82: 357–385
- Gareau JR, Lima CD (2010) The SUMO pathway: emerging mechanisms that shape specificity, conjugation and recognition. *Nat Rev Mol Cell Biol* 11: 861–871
- Geiss-Friedlander R, Melchior F (2007) Concepts in sumoylation: a decade on. *Nat Rev Mol Cell Biol* 8: 947–956
- Godoy P, Hewitt NJ, Albrecht U, Andersen ME, Ansari N, Bhattacharya S, Bode JG, Bolleyen J, Borner C, Böttger J et al (2013) Recent advances in 2D and 3D in vitro systems using primary hepatocytes, alternative hepatocyte sources and non-parenchymal liver cells and their use in investigating mechanisms of hepatotoxicity, cell signaling and ADME. *Arch Toxicol* 87: 1315–1330
- Goodwin B, Redinbo MR, Kliewer SA (2002) Regulation of cyp3a gene transcription by the pregnane x receptor. *Annu Rev Pharmacol Toxicol* 42: 1–23
- Goto T, Elbahrawy A, Furuyama K, Horiguchi M, Hosokawa S, Aoyama Y, Tsuboi K, Sakikubo M, Hirata K, Masui T et al (2017) Liver-specific Prox1

- inactivation causes hepatic injury and glucose intolerance in mice. *FEBS Lett* 591: 624–635
- Hendriks IA, Vertegaal AC (2016) A comprehensive compilation of SUMO proteomics. *Nat Rev Mol Cell Biol* 17: 581–595
- Hendriks IA, Lyon D, Su D, Skotte NH, Daniel JA, Jensen LJ, Nielsen ML (2018) Site-specific characterization of endogenous SUMOylation across species and organs. *Nat Commun* 9: 2456
- Hofmann AF (1989) Current concepts of biliary secretion. *Dig Dis Sci* 34: 16s–20s
- Hofmann AF (2007) Biliary secretion and excretion in health and disease: current concepts. *Ann Hepatol* 6: 15–27
- Honda A, Salen G, Matsuzaki Y, Batta AK, Xu G, Leitersdorf E, Tint GS, Erickson SK, Tanaka N, Shefer S (2001) Side chain hydroxylations in bile acid biosynthesis catalyzed by CYP3A are markedly up-regulated in Cyp27^{-/-} mice but not in cerebrotendinous xanthomatosis. *J Biol Chem* 276: 34579–34585
- Jumper J, Evans R, Pritzel A, Green T, Figurnov M, Ronneberger O, Tunyasuvunakool K, Bates R, Žídek A, Potapenko A et al (2021) Highly accurate protein structure prediction with AlphaFold. *Nature* 596: 583–589
- Juza RM, Pauli EM (2014) Clinical and surgical anatomy of the liver: a review for clinicians. *Clin Anat* 27: 764–769
- Kim D-H, Xiao Z, Kwon S, Sun X, Ryerson D, Tkac D, Ma P, Wu S-Y, Chiang C-M, Zhou E et al (2015) A dysregulated acetyl/SUMO switch of FXR promotes hepatic inflammation in obesity. *EMBO J* 34: 184–199
- Lazaridis KN, Pham L, Tietz P, Marinelli RA, deGroen PC, Levine S, Dawson PA, LaRussa NF (1997) Rat cholangiocytes absorb bile acids at their apical domain via the ileal sodium-dependent bile acid transporter. *J Clin Invest* 100: 2714–2721
- Lee GY, Jang H, Lee JH, Huh JY, Choi S, Chung J, Kim JB (2014) PIASy-mediated sumoylation of SREBP1c regulates hepatic lipid metabolism upon fasting signaling. *Mol Cell Biol* 34: 926–938
- Li T, Chiang JY (2013) Nuclear receptors in bile acid metabolism. *Drug Metab Rev* 45: 145–155
- Love MI, Huber W, Anders S (2014) Moderated estimation of fold change and dispersion for RNA-seq data with DESeq2. *Genome Biol* 15: 550
- Lu Z, Priya Rajan SA, Song Q, Zhao Y, Wan M, Aleman J, Skardal A, Bishop C, Atala A, Lu B (2021) 3D scaffold-free microlivers with drug metabolic function generated by lineage-reprogrammed hepatocytes from human fibroblasts. *Biomaterials* 269: 120668
- Mahajan R, Delphin C, Guan T, Gerace L, Melchior F (1997) A small ubiquitin-related polypeptide involved in targeting RanGAP1 to nuclear pore complex protein RanBP2. *Cell* 88: 97–107
- Matunis MJ, Coutavas E, Blobel G (1996) A novel ubiquitin-like modification modulates the partitioning of the Ran-GTPase-activating protein RanGAP1 between the cytosol and the nuclear pore complex. *J Cell Biol* 135: 1457–1470
- Meulmeester E, Kunze M, Hsiao HH, Urlaub H, Melchior F (2008) Mechanism and consequences for paralog-specific sumoylation of ubiquitin-specific protease 25. *Mol Cell* 30: 610–619
- Oteng AB, Higuchi S, Banks AS, Haeusler RA (2021) Cyp2c-deficiency depletes muricholic acids and protects against high-fat diet-induced obesity in male mice but promotes liver damage. *Mol Metab* 53: 101326
- Ouyang H, Qin Y, Liu Y, Xie Y, Liu J (2013) Prox1 directly interacts with LSD1 and recruits the LSD1/NuRD complex to epigenetically co-repress CYP7A1 transcription. *PLoS One* 8: e62192
- Pan M-R, Chang T-M, Chang H-C, Su J-L, Wang H-W, Hung W-C (2009) Sumoylation of Prox1 controls its ability to induce VEGFR3 expression and lymphatic phenotypes in endothelial cells. *J Cell Sci* 122: 3358–3364
- Panda S, Antoch MP, Miller BH, Su AI, Schook AB, Straume M, Schultz PG, Kay SA, Takahashi JS, Hogenesch JB (2002) Coordinated transcription of key pathways in the mouse by the circadian clock. *Cell* 109: 307–320
- Perez-Riverol Y, Bai J, Bandla C, García-Seisdedos D, Hewapathirana S, Kamatchinathan S, Kundu DJ, Prakash A, Frericks-Zipper A, Eisenacher M et al (2022) The PRIDE database resources in 2022: a hub for mass spectrometry-based proteomics evidences. *Nucleic Acids Res* 50: D543–D552
- Perreault M, Wunsch E, Bialek A, Trottier J, Verreault M, Caron P, Poirier GG, Milkiewicz P, Barbier O (2018) Urinary elimination of bile acid glucuronides under severe cholestatic situations: contribution of hepatic and renal glucuronidation reactions. *Can J Gastroenterol Hepatol* 2018: 8096314
- Pichler A, Knipscheer P, Saitoh H, Sixma TK, Melchior F (2004) The RanBP2 SUMO E3 ligase is neither HECT- nor RING-type. *Nat Struct Mol Biol* 11: 984–991
- Pichler A, Knipscheer P, Oberhofer E, van Dijk WJ, Körner R, Olsen JV, Jentsch S, Melchior F, Sixma TK (2005) SUMO modification of the ubiquitin-conjugating enzyme E2-25K. *Nat Struct Mol Biol* 12: 264–269
- Qin J, Gao D-m, Jiang Q-F, Zhou Q, Kong Y-Y, Wang Y, Xie Y-H (2004) Prospero-related homeobox (Prox1) is a corepressor of human liver receptor homolog-1 and suppresses the transcription of the cholesterol 7- α -hydroxylase gene. *Mol Endocrinol* 18: 2424–2439
- Rosonina E, Akhter A, Dou Y, Babu J, Sri Theivakadadham VS (2017) Regulation of transcription factors by sumoylation. *Transcription* 8: 220–231
- Shan S-f, Wang L-f, Zhai J-w, Qin Y, Ouyang H-f, Kong Y-y, Liu J, Wang Y, Xie Y-h (2008) Modulation of transcriptional corepressor activity of prospero-related homeobox protein (Prox1) by SUMO modification. *FEBS Lett* 582: 3723–3728
- Si-Tayeb K, Lemaigre FP, Duncan SA (2010) Organogenesis and development of the liver. *Dev Cell* 18: 175–189
- Sosa-Pineda B, Wigle JT, Oliver G (2000) Hepatocyte migration during liver development requires Prox1. *Nat Genet* 25: 254–255
- Staelens B, Fonseca VA (2009) Bile acids and metabolic regulation: mechanisms and clinical responses to bile acid sequestration. *Diabetes Care* 32(Suppl 2): S237–S245
- van de Steeg E, Wagenaar E, van der Kruijssen CMM, Burggraaff JEC, de Waart DR, Elferink RPJO, Kenworthy KE, Schinkel AH (2010) Organic anion transporting polypeptide 1a/1b-knockout mice provide insights into hepatic handling of bilirubin, bile acids, and drugs. *J Clin Invest* 120: 2942–2952
- Stein S, Oosterveer MH, Mataki C, Xu P, Lemos V, Havinga R, Dittner C, Ryu D, Menzies KJ, Wang X et al (2014) SUMOylation-dependent LRH-1/PROX1 interaction promotes atherosclerosis by decreasing hepatic reverse cholesterol transport. *Cell Metab* 20: 603–613
- Straniero S, Laskar A, Savva C, Härdfeldt J, Angelin B, Rudling M (2020) Of mice and men: murine bile acids explain species differences in the regulation of bile acid and cholesterol metabolism. *J Lipid Res* 61: 480–491
- Tatham MH, Jaffray E, Vaughan OA, Desterro JMP, Botting CH, Naismith JH, Hay RT (2001) Polymeric chains of SUMO-2 and SUMO-3 are conjugated to protein substrates by SAE1/SAE2 and Ubc9. *J Biol Chem* 276: 35368–35374
- Treuter E, Venteclef N (2011) Transcriptional control of metabolic and inflammatory pathways by nuclear receptor SUMOylation. *Biochim Biophys Acta* 1812: 909–918
- Varadi M, Anyango S, Deshpande M, Nair S, Natassia C, Yordanova G, Yuan D, Stroe O, Wood G, Laydon A et al (2022) AlphaFold protein structure database: massively expanding the structural coverage of protein-

- sequence space with high-accuracy models. *Nucleic Acids Res* 50: D439–D444
- Velazquez JJ, LeGraw R, Moghadam F, Tan Y, Kilbourne J, Maggiore JC, Hislop J, Liu S, Cats D, de Sousa C et al (2021) Gene regulatory network analysis and engineering directs development and vascularization of multilineage human liver organoids. *Cell Syst* 12: 41–55.e11
- Vertegaal ACO (2022) Signalling mechanisms and cellular functions of SUMO. *Nat Rev Mol Cell Biol* 23: 715–731
- Wang DQ, Tazuma S, Cohen DE, Carey MC (2003) Feeding natural hydrophilic bile acids inhibits intestinal cholesterol absorption: studies in the gallstone-susceptible mouse. *Am J Physiol Gastrointest Liver Physiol* 285: G494–G502
- Werner A, Moutty M-C, Möller U, Melchior F (2009) Performing *in vitro* sumoylation reactions using recombinant enzymes. In *SUMO protocols*, Ulrich HD (ed), pp 187–199. Totowa, NJ: Humana Press
- Xia X, Francis H, Glaser S, Alpini G, LeSage G (2006) Bile acid interactions with cholangiocytes. *World J Gastroenterol* 12: 3553–3563
- Xie W, Radominska-Pandya A, Shi Y, Simon CM, Nelson MC, Ong ES, Waxman DJ, Evans RM (2001) An essential role for nuclear receptors SXR/PXR in detoxification of cholestatic bile acids. *Proc Natl Acad Sci USA* 98: 3375–3380
- Xu C, Li CY, Kong AN (2005) Induction of phase I, II and III drug metabolism/transport by xenobiotics. *Arch Pharm Res* 28: 249–268
- Zhu J, Zhu S, Guzzo CM, Ellis NA, Sung KS, Choi CY, Matunis MJ (2008) Small ubiquitin-related modifier (SUMO) binding determines substrate recognition and paralog-selective SUMO modification. *J Biol Chem* 283: 29405–29415
- Zhu S, Goeres J, Sixt KM, Békés M, Zhang X-D, Salvesen GS, Matunis MJ (2009) Protection from isopeptidase-mediated deconjugation regulates paralog-selective sumoylation of RanGAP1. *Mol Cell* 33: 570–580



License: This is an open access article under the terms of the [Creative Commons Attribution-NonCommercial-NoDerivs License](#), which permits use and distribution in any medium, provided the original work is properly cited, the use is non-commercial and no modifications or adaptations are made.